October 2017

Cell Division Regulation in Staphylococcus aureus

Catherine M. Spanoudis
University of South Florida, cathyspanoudis@yahoo.com

Cell Division Regulation in *Staphylococcus aureus*

by

Catherine M. Spanoudis

A thesis submitted in partial fulfillment
of the requirements for the degree of
Master of Science in Microbiology
Department of Cell Biology, Microbiology & Molecular Biology
College of Arts and Sciences
University of South Florida

Major Professor: Prahathees Eswara, Ph.D.
Lindsey Shaw, Ph.D.
Stanley Stevens, Ph.D.

Date of Approval:
October 17, 2017

Keywords: GpsB, Fluorescence Microscopy, Mass Spectrometry

DEDICATION

I dedicate my thesis work to my amazing parents. Thank you for supporting me throughout the years. Without your love, guidance, and words of encouragement I would not be where I am today. I appreciate and am eternally grateful for everything you have done for me.

ACKNOWLEDGEMENTS

I would like to thank my advisor and mentor, Dr. Prahathees Eswara. Thank you for accepting me into your lab and giving me this amazing opportunity. You have taught me so much during my time here and all your guidance was greatly appreciated. Thank you for pushing me, for truly caring about your graduate students, and for introducing me to the field of bacterial cell division. Additionally, I would like to thank my committee members, Dr. Lindsey Shaw and Dr. Stanley Stevens for all the feedback they provided throughout my time here.

I would also like to recognize the members of Riordan and Shaw labs for all their help. Thank you for taking the time to teach me new techniques and for all your assistance throughout this degree. Finally, I would like to acknowledge all the volunteers, our lab technician, Gianni Graham, and my fellow lab members: Robert Brzozowski, Ryan Henry, Julia Banek and Sameeksha Alva. I appreciate all your aid and for creating an amazing work environment. I will truly miss working with all of you.

Finally, I would like to thank Dr. Dale Chaput for all her assistance preparing samples for mass spectrometry at the Center for Drug Discovery and Innovation (CDDI). Thank you for taking the time to teach me.

TABLE OF CONTENTS

LIST OF TABLES

LIST OF FIGURES

ABSTRACT

Cell division is a fundamental biological process that occurs in all kingdoms of life. Our understanding of cell division in bacteria stems from studies in the rod-shaped model organisms: Gram-negative *Escherichia coli* and Gram-positive *Bacillus subtilis*. The molecular underpinnings of cell division regulation in non-rod-shaped bacteria remain to be studied in detail. Rod-shaped bacteria possess many positive and negative regulatory proteins that are essential to the proper placement of the division septa and ultimately the production of two identical daughter cells, many of which are absent in cocci. Given that essential cell division proteins are attractive antibacterial drug targets, it is imperative for us to identify key cell division factors especially in pathogens, to help counter the emergence of multi-drug resistance. In *Staphylococcus aureus*, a spherical Gram-positive opportunistic pathogen that causes a range of diseases from minor skin infections to life-threatening sepsis, we have identified the role of an essential protein, GpsB, in the regulation of cell division. We discovered that GpsB preferentially localizes to cell division sites and that overproduction of GpsB results in cell enlargement typical of FtsZ inhibition, while depletion of GpsB results in cell lysis and nucleoid-less minicell formation. The identification of GpsB's interaction partners will allow us to understand the molecular mechanism by which GpsB regulates cell division.

INTRODUCTION

Cell Division and its Regulators in Model Organisms

Cell division is an essential process that involves cell elongation, DNA replication, and septum formation [1]. Usually, in bacteria, this process leads to the formation of two identical daughter cells. During septum formation FtsZ, an essential cell division protein, polymerizes into a ring-like structure commonly referred to as the Z-ring, at midcell [2]. FtsZ shares structural homology with eukaryotic tubulin and is involved in membrane constriction [3]. The Z-ring also acts as a scaffold and recruits other cell division proteins to the septa [1]. This complex of over a dozen proteins at the division septa constitutes a structure commonly referred to as the divisome [5]. A common question that therefore arises, is how FtsZ knows where midcell is located.

In *Escherichia coli*, a Gram-negative rod-shaped model organism, there are two known systems that regulate Z-ring placement: the Min system and the nucleoid occlusion system **(Fig. 1)** [4]. The Min system is highly dynamic and is comprised of three proteins: MinC, MinD, and MinE, which work together to prevent Z-ring assembly at the cell poles [6,7]. MinC is an inhibitor of FtsZ and is recruited to the membrane by MinD [6]. MinE then activates the MinD ATPase which results in the oscillation of the MinCD complex from one pole of the cell to the other [6]. This oscillatory system confines Z-ring assembly to midcell, limiting aberrant assembly at the poles. Additionally, the nucleoid occlusion system negatively regulates Z-ring assembly by preventing its polymerization over the DNA [8]. This system is comprised of the DNA-binding protein, SlmA [9]. SlmA binds to SlmA-binding sequences along the chromosome; this interaction then allows for FtsZ inhibition by preventing it from polymerizing [8-11]. While these

systems work together in *E. coli* to ensure proper placement of the Z-ring, the regulation of division septa placement varies from organism to organism [7]. For instance, in *Bacillus subtilis*, a Gram-positive rod, the nucleoid occlusion system is present, but functions in a different manner [9]. In *B. subtilis*, the Noc protein binds to Noc binding sequences within the chromosome and to the cell membrane using an N-terminal amphipathic helix [19]. These Noc-DNA complexes physically prevent the assembly of the Z-ring over the nucleoid further preventing FtsZ ring formation at sites other than midcell [19]. Additionally, unlike in *E. coli*, the Min system does not oscillate. Instead, another cell division protein, DivIVA, recruits the MinCD complex to the division septa through MinJ **(Fig. 1)** [12-15]. MinJ and DivIVA form double rings directly adjacent to sites of active division; MinCD is subsequently recruited to these rings [14,15]. This arrangement allows for spatial regulation of the MinCD complex by separating it from FtsZ, allowing the Z-ring to form at midcell [15]. Collectively, these negative regulators prevent abnormal assembly of Z-rings directly adjacent to a newly formed septum [12-15]. While the Min and nucleoid occlusion systems are present in the aforementioned rod-shaped organisms, they are largely absent among organisms exhibiting other cellular morphologies, such as cocci and ovoid-shaped microbes [16]. While *Staphylococcus aureus*, a Gram-positive spherical organism, possesses a *noc* homolog that plays a role in inhibiting Z-ring placement over the DNA, it is amongst the organisms that do not possess a Min system [17, 20]. It was also found that a *divIVA* knock-out mutation did not affect cell division or chromosome segregation [17]. However, a DivIVA-like protein, GpsB, is present in *S. aureus* and other clinically relevant Gram-positive microbes [18]. Thus, it is possible that GpsB plays a role in regulating Z-ring assembly and/or placement in *S. aureus*.

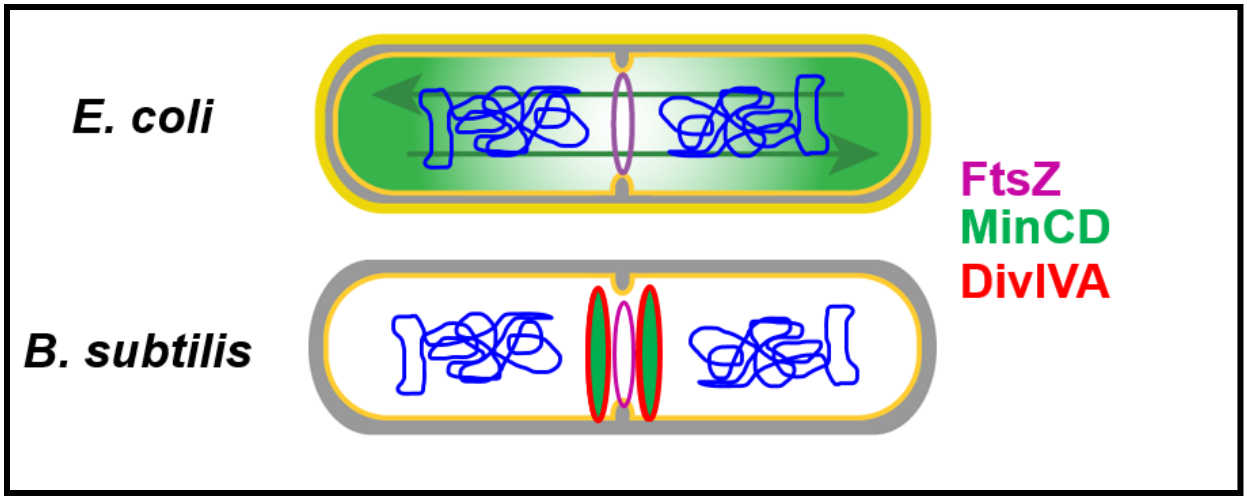

Figure 1- Cell Division Regulation in *Escherichia coli* and *Bacillus subtilis*
There are two known systems that regulate Z-ring placement: the nucleoid occlusion system and the Min system. In *E. coli,* the Min system is an oscillatory system that prevents Z-ring assembly at cell poles and the nucleoid occlusion system prevents ring formation over the DNA [7]. In *B. subtilis* the nucleoid occlusion system is present and appears to perform a role similar to that in *E. coli*. However, unlike *E. coli*, the Min system does not oscillate and is recruited to the division septa by DivIVA [14].

Identification of GpsB and Observations in *B. subtilis*

GpsB, formerly called YpsB, was first identified in *B. subtilis* [18, 21]. Extensive sequence alignments and phylogenetic analysis revealed that YpsB is a paralog of DivIVA [18, 21]. This ninety-eight amino acid long protein was found to have a coiled-coil region (amino acids 32-70) that shares some similarity with DivIVA [18, 21]. It was also observed that the N-terminal region of YpsB, which consists of approximately thirty amino acids, exhibits a high degree of similarity to that of DivIVA [18, 21]. While both proteins localize to the nascent septa during division, their involvement in cell division and localization patterns differ [18,21]. DivIVA is a negative-curvature sensing protein that forms rings near the active division septa and patches at cell poles upon the completion of a round of division [14]. YpsB on the other hand shuttles between the lateral cell walls (during elongation) and the division septa (once the Z-ring forms) [21]. Additionally, YpsB did not appear to be involved in division site selection and was only essential in *B. subtilis* cells lacking FtsA, a Z-ring membrane anchor, or EzrA, a negative

regulator of FtsZ ring assembly, and in high salt conditions [18, 21, 22]. YpsB was also found to be involved in shuttling the penicillin-binding protein PBP1, which exhibits both transglycosylase and transpeptidase activity during peptidoglycan synthesis [21, 22]. This observation resulted in YpsB being renamed GpsB (Guiding Penicillin Binding Protein 1 Shuttling Protein) [21].

Crystal Structure of GpsB and its Role in *Listeria monocytogenes*

Listeria monocytogenes, a Gram-positive rod-shaped organism, is a foodborne pathogen that can cause life-threatening illnesses that range from sepsis to meningoencephalitis [23]. *L. monocytogenes* is therefore a clinically relevant organism and GpsB is conserved in it. In *L. monocytogenes*, GpsB is a one-hundred and thirteen amino acid long protein that shares 56.7% sequence identity with *B. subtilis* GpsB and possesses the highly conserved N-terminus [22]. The crystal structure of GpsB was determined in *L. monocytogenes* and *B. subtilis* **(Fig. 2)**. The N-terminal domain (amino acids 1-73) of GpsB in *L. monocytogenes* forms a dimer made of two identical subunits composed of two α-helices [22]. In *B. subtilis*, the N-terminus (amino acids 1-68) of GpsB also forms dimers [22]. The C-terminal domain of GpsB forms trimers in both organisms [22]. Full length GpsB is hexameric; there are three N-terminal dimers and two C-terminal timers that make up the structure [22]. Hexamerization was also found to be important for function; mutations that affect C-terminal trimerization result in increased cell lysis [22].

In *L. monocytogenes*, GpsB alternates between the lateral walls and the division septa sites of active peptidoglycan synthesis, similar to GpsB in *B. subtilis* [22]. To determine its essentiality, a *gpsB* knockout mutant was observed and it exhibited severe lysis, division abnormalities, and growth defects [22]. These knockout phenotypes were found to be associated with abnormal cell wall synthesis suggesting that like *B. subtilis*, GpsB may interact with PBPs in *L. monocytogenes* [22]. Further experimentation revealed that the bifunctional PBP A1, an ortholog of PBP1 in *B. subtilis*, was dysregulated in the absence of GpsB, indicating that

GpsB is involved in shuttling the protein [22]. Deletion of *pbpA1* suppressed the *gpsB* knockout phenotype, providing additional support for PBP A1's uncontrolled activity in GpsB's absence [22]. Additionally, *in vivo* studies showed an attenuation in virulence in a *gpsB* deletion mutant [22]. The reduced virulence was similar to that of the pathogenicity island LIPI-1 mutant, which encodes six of *L. monocytogenes's* main virulence factors [24]. GpsB is therefore essential in *L. monocytogenes* and shares structural and functional components of *B. subtilis's* GpsB.

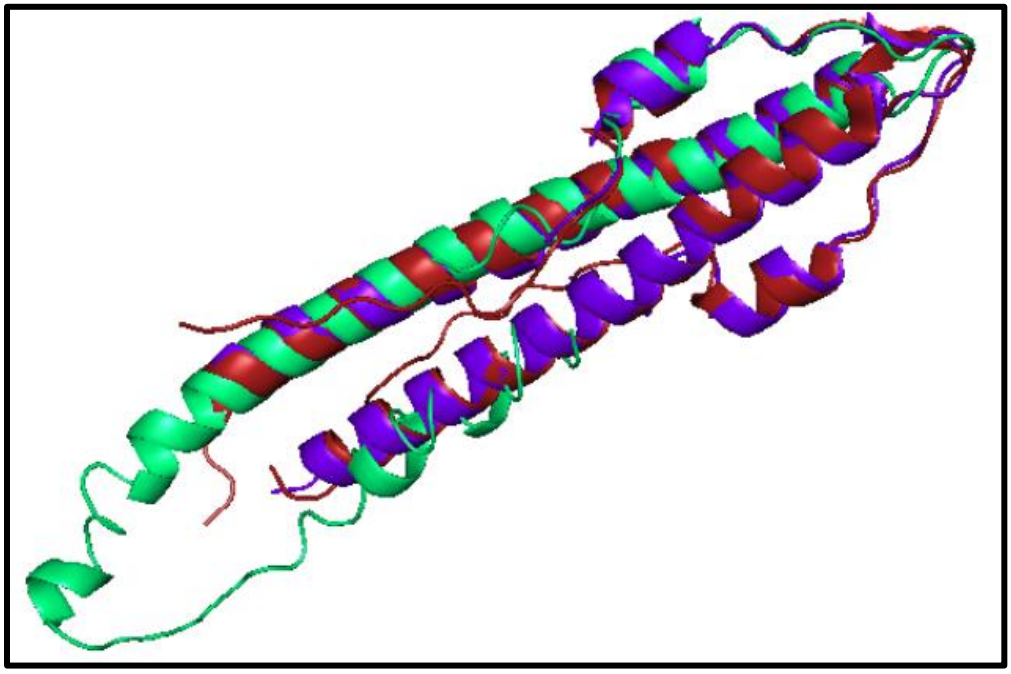

Figure 2- Structures of N-terminal Domain of GpsB in Listeria monocytogenes, Bacillus subtilis, and Staphylococcus aureus
GpsB from *L. monoctyogenes* (Red) shares 56.7% sequence identity with *B. subtilis* GpsB (Purple) and 43% sequence identity with *S aureus* GpsB (Green). The published crystal structures of the N-terminal domains from *Listeria* and *Bacillus* were found to form dimers [22]. The predicted structure of *S. aureus's* GpsB was generated using I-TASSER and aligned using PyMOL and appears to have structural similarities.

Role of GpsB in *Streptococcus pneumoniae*

Streptococcus pneumoniae is an ovoid-shaped Gram-positive organism that can cause life-threatening illnesses ranging from pneumonia to sepsis to meningitis [25]. GpsB is conserved in this organism and it is an essential protein in some strain backgrounds [26, 28].

Depletion of GpsB leads to the formation of enlarged cells with unsegregated DNA, cells with many unconstricted rings, and ultimately cell lysis [26]. These phenotypes are similar to what was observed when the monofunctional PBP, Pbp2x, was selectively inhibited my methicillin; this suggested that GpsB, like Pbp2x, is involved in septal ring closure and septal peptidoglycan synthesis [26, 27]. GpsB and FtsZ have unique patterns of localization with some overlap; GpsB can reside in locations not occupied by FtsZ [26]. Since multiple unconstricted rings of division proteins, such as FtsZ, Pbp2x, and Pbp1a (a bifunctional PBP) were observed in GpsB depleted cells, GpsB is not necessary for ring formation [26]. GpsB is therefore necessary for maintenance of the ovococci cell shape in *S. pneumoniae* and plays a role in proper septal ring closure.

Essentiality and Localization of GpsB in *Staphylococcus aureus*

In *S. aureus*, GpsB is a one hundred and fourteen amino acid long protein and little is known about its role or roles in cell division. *gpsB* was reported to be a domain-essential gene based on transposon mutagenesis; the DivIVA-like N-terminal domain appears to be essential [47]. It was observed that GpsB localizes to the division septa and forms what appears to be a ring or disk [48]. The interaction between GpsB and EzrA that occurs in *B. subtllis* is proposed to be conserved in *S. aureus* [49]. In cells depleted of EzrA, GpsB becomes delocalized suggesting that EzrA is involved in its recruitment to the division septa [48].

Serine/Threonine Protein Kinases

Protein phosphorylation was primarily studied in eukaryotic organisms, but over the years it has become evident that phosphorylation is prevalent among Bacteria. In Eukaryotes, phosphorylation occurs on only a few residues while in Bacteria, there are a much larger array of residues. [29]. Most prokaryotic Phyla possess kinases that share structural similarities to

eukaryotic kinases, making them “eukaryotic-like” [29, 32, 33]. These eukaryotic-like kinases are predominately involved in phosphorylating serine and threonine resides, which is why they are referred to as eukaryotic serine/ threonine kinases (eSTKs) [29]. eSTKs have an intracellular catalytic kinase domain and most have an extracellular regulatory domain [29]. These kinases are of great interest because they were found to be involved in regulating everything from virulence to cell division to metabolism. [30-33]. Most of what is known about eSTKs comes from studies utilizing model organisms, which include: *B. subtilis*, *S. aureus*, *S. pneumoniae*, and *Mycobacterium tuberculosis*.

In *B. subtilis*, the eSTK PrkC is required for sporulation and biofilm formation and is involved in metabolism and maintenance of cell wall architecture through the phosphorylation of many proteins, including GpsB [34-38]. GpsB is part of a negative feedback loop and is involved in the autophosphorylation, activation, and inactivation of PrkC [39]. While PrkC is not directly involved with cell division, its interaction with cell division proteins is vital to proper functioning in *B. subtilis*. *S. aureus* also possesses eSTKs, such as Stk1 [29, 33]. While no cell division proteins have been reported to be phosphorylated by Stk1, some evidence suggests it could participate in cell wall synthesis [29]. Stk1 phosphorylates proteins involved in everything from antibiotic resistance to cell wall metabolism regulation to biofilm and toxin production [29-31, 33]. While more research needs to be done to determine if eSTKs are involved in regulating cell division, current research highlights their importance in *S. aureus’s* virulence.

Additionally, StkP is an eSTK in *S. pneumoniae.* The first inclination that StkP was involved in cell division and cell shape maintenance was observed in *stkP* deficient cells that became elongated and no longer appeared ovoid in shape [40]. Unlike *B. subtilis*, GpsB is not phosphorylated, but it is required for the localization of StkP [41]. While StkP may phosphorylate other cell division and morphology regulators, current observations show that eSTK activity is quintessential to maintaining *S. pneumoniae’s* ovoid shape and producing two identical

daughter cells. Finally, *M. tuberculosis*, has eleven eSTKs (PknA through PknL) [42]. Some of these eSTKs are essential and play roles in cell division, polar peptidoglycan synthesis, DNA condensation and virulence [29, 33, 43, 44-46]. More research need to be done to determine attentional roles and links to cell division and/or morphogenesis.

MATERIALS AND METHODS

Media

All media was made using deionized water and autoclaved for sterility. Antibiotics were added at the following concentrations:

Table 1- Antibiotic Concentrations

Antibiotics	Final Concentration
Bacillus subtilis	
Spectinomycin (Spec)	100 µg mL^{-1}
Chloramphenicol (Chlor)	5 µg mL^{-1}
Tetracycline (Tet)	10 µg mL^{-1}
Kanamycin (Kan)	5 µg mL^{-1}
Erythromycin (Erm)	5 µg mL^{-1}
Staphylococcus aureus	
Chloramphenicol	5 µg mL^{-1}
Erythromycin	5 µg mL^{-1}
Escherichia coli	
Ampicillin (Amp)	100 µg mL^{-1}
Kanamycin	50 µg mL^{-1}

Tryptic Soy Agar (TSA)

Tryptone 15 g L^{-1}

Soytone 5 g L^{-1}

NaCl	5 g L^{-1}
Agar	15 g L^{-1}

Tryptic Soy Broth (TSB)

Tryptone	17 g L^{-1}
Soytone	3 g L^{-1}
Dextrose	2.5 g L^{-1}
NaCl	5 g L^{-1}
Dibasic potassium phosphate (K_2HPO_4)	2.5 g L^{-1}

Luria-Bertani Agar (LBA)

Tryptone	10 g L^{-1}
Yeast extract	10 g L^{-1}
NaCl	10 g L^{-1}
Agar	15 g L^{-1}

Luria-Bertani Broth (LB)

Tryptone	10 g L^{-1}
Yeast extract	10 g L^{-1}
NaCl	10 g L^{-1}

Isolation of Genetic Material

Plasmid Purification

Strains were struck out on appropriate antibiotic containing media for single colony isolation and placed in 37°C incubator overnight. 5 mL of broth was then inoculated with a

colony and grown overnight. Plasmids were purified following the protocol in the QIAprep Spin Miniprep Kit (Qiagen).

Chromosomal DNA Extractions

1X TE Buffer

1M Tris-HCl (pH 8.0)	10 mL
0.5M EDTA (pH 8.0)	2 mL
ddH_2O	988 mL

Lysis Buffer

50mM NaH_2PO_4

300mM NaCl

Adjust pH to 8.0

* 2.5% Lysozyme added to make lysis buffer with lysozyme (10 mg mL^{-1} stock solution)

Strains were struck out on appropriate antibiotic containing media for single colony isolation and placed in 37°C incubator overnight. 10 mL culture was grown overnight in LB with the appropriate antibiotic in 37°C incubator. The cultures were spun down and resuspended in 1 mL of lysis buffer. Samples were spun down again and resuspended in 500 µL of lysis buffer with lysozyme. Samples were then placed in a 37°C incubator for 15 min. 50 µl of 20% Sarkosyl chromosomal DNA was added and then the samples were incubated at 37°C for 5 min. 500 µl of phenol chloroform was added and the sample was vortexed until it turned milky white. Spin down samples at 13,000 rpm for 10 min. The top (clear) layer was then removed and placed into a new tube along with 50 µl of 3M sodium acetate. 1 ml of 100% ethanol was then added. DNA was removed from the tube and placed into a new tube. 1 ml of 70% ethanol is added to the tube with DNA. The sample was spun down at 13,000 rpm and the supernatant was

removed. Samples were then incubated in a 37°C incubator (~1hr). 250-300 µl of 1X TE buffer was added to dissolve pellet of DNA.

Competent Cells

DH5α (*E. coli*)

TC Buffer

10mM Tris-HCl (pH 8.0)	1 mL
50mM $CaCl_2$	5 mL
ddH_2O	94 mL

TCG Buffer

10mM Tris-HCl (pH 8.0)	1 mL
50mM $CaCl_2$	5 mL
20% Glycerol	40 mL
ddH_2O	54 mL

DH5a *E. coli* strain was streaked out for single colony isolation and incubated overnight at 37°C. 20 mL LB inoculated with colony and grown to OD_{600}=0.5. Culture diluted to OD_{600}=0.05 in fresh LB. At OD_{600}=0.4 cultures transferred to ice for 10min. Cells were spun down. Pellet resuspended in 12.5 mL TC buffer and placed on ice for 15min. Cells spun down and resuspended in 3.25 mL TCG and stored in aliquots at -80°C.

PY79 (*B. subtilis*)

SpC Media

1X T-base	100 mL
50% Glucose	1 mL

1.2% $MgSO_4$	1 mL
10% Yeast extract	2 mL
1% Casamino acids	2.5 mL

SpII Media

1X T-base	100 mL
50% Glucose	1 mL
1.2% $MgSO_4$	7 mL
0.1M $CaCl_2$	0.5 mL
10% Yeast extract	1 mL
1% Casamino acids	1 mL

PY79 *B. subtilis* strain was streaked out for single colony isolation and grown overnight at 37°C. 20 mL of SpC media was inoculated with a single colony. Grow until cells enter stationary phase (4-6hr). Dilute 1:10 into prewarmed SpII media and incubate for 90 min. at 37°C. Spin down and save supernatant. Resuspend pellet in 1.6 mL of saved supernatant and 0.4 mL of 50% glycerol. Store aliquots at -80°C.

RN4220 (*S. aureus*)

RN4220 *S. aureus* strain was streaked out for single colony isolation and grown overnight at 37°C. A 10 mL culture was grown overnight and diluted into fresh media to a volume of 10 mL and an OD_{600} of 0.5. Culture grown for 30 min. All subsequent steps performed on ice. Cultures pelleted and resuspended in 10 mL of cold sterile H_2O twice. Pellet resuspended in 1 mL of 10% glycerol and then spun down. Pellet then resuspended in 400 µL of 10% glycerol and spun down. Pellet was then resuspended in 200 µL of 10% glycerol and aliquots were stored at -80°C.

Transformations

DH5α (*E. coli*)

DH5α competent cells were thawed on ice and 80 µL were added to ligated DNA. Incubated on ice for 1 hr. and then heat shocked at 42°C for 1 min. Incubated on ice for 1 min. and then transferred to test tube containing 1 mL LB. Incubated at 37°C for 1 hr., spun down, and plated on LBA with correct antibiotic.

BL21-DE3 (*E. coli*)

BL21-DE3 competent cells were thawed on ice and 50 µL were added to 10 µL of purified plasmid. Incubated on ice for 1 hr. and then heat shocked at 42°C for 1 min. Incubated on ice for 1 min. and then transferred to test tube containing 1 mL LB. Incubated at 37°C for 1 hr., spun down, and plated on LBA with correct antibiotic.

PY79 (*B. subtilis*)

SpII-EGTA

1X T-base	10 mL
50% Glucose	0.1 mL
1.2% $MgSO_4$	0.7 mL
10% Yeast extract	0.1 mL
1% Casamino acids	0.1 mL
0.1M EGTA	0.2 mL

PY79 competent cells thawed on ice. 80 µL of competent cells, 10 µL of DNA, and 80 µL of SpII-EGTA incubated in a test tube at 37°C for 40 min. Contents of test tube plated on LBA containing appropriate antibiotic.

RN4220 (*S. aureus*)

RN4220 competent cells thawed on ice for 5 min. and then at room temperature for 5 min. Cells spun down and resuspended in 50 µL of 10% glycerol with 500mM sucrose. DNA added and everything was transferred to a 1 mm electroporation cuvette and pulsed once at 1850V. 1 mL of TSB supplemented with 500mM sucrose was used to transfer contents of cuvette to a class test tube, which was incubated at 37°C for 1 hr. Culture was spun down and plates on TSA plates containing the appropriate antibiotic.

Transductions

SH1000 (*S. aureus*)

Phage Buffer

$MgSO_4$	0.25 g L^{-1}
$CaCl_2$	0.59 g L^{-1}
Tris-HCl (pH 7.8)	6.06 g L^{-1}
NaCl	5.9 g L^{-1}
Gelatin	1 g L^{-1}

Phage lysate made by growing overnight culture of strain of interest in RN4220. Overnight culture diluted to an OD_{600}=0.1 into 5 mL of TSB and 5mL of phage buffer. 250 µL of Φ11 phage lysate was then added and lysate was incubated at 30°C and then filter sterilized. 1 mL of an overnight SH1000 culture was added to 15 mL falcon tubes along with 12 µL of 1M $CaCl_2$. 500 µL of phage lysate was added to first tube, 100 µL added to second tube and none

added to third tube. Tubes were incubated at 37°C for 15 min. 2 mL of 1% sodium citrate was added to each tube and centrifuged for 10 min at 4150 rpm. Pellet resuspended in TSB supplemented with 1% sodium citrate and incubated at 37°C for 1 hr. Tubes spun down for 10 min at 4150 rpm, resuspended in 200 µL of TSB with 1% sodium citrate, and plated on media containing appropriate antibiotic.

Protein Purification

Lysis Buffer

1M NaCl	300 mL L^{-1}
0.5M NaH_2PO_4	100 mL L^{-1}

Wash Buffer #1 (20mM Imidazole)

1M NaCl	300 mL L^{-1}
0.5M NaH_2PO_4	100 mL L^{-1}
1M Imidazole	20 mL L^{-1}

Wash Buffer #2 (80mM Imidazole)

1M NaCl	300 mL L^{-1}
0.5M NaH_2PO_4	100 mL L^{-1}
1M Imidazole	80 mL L^{-1}

Elution Buffer (250mM Imidazole)

1M NaCl	300 mL L^{-1}
0.5M NaH_2PO_4	100 mL L^{-1}
1M Imidazole	250 mL L^{-1}

Overnight culture of BL21-DE3 strain containing 6X histidine-tagged protein of interest was made. Overnight culture was diluted 1:20 into 500 mL of fresh media and grown to OD_{600}= 0.5. Appropriate inducer was then added, and culture was grow for 4 hr. and pelleted. Pellet washed with lysis buffer twice and then resuspended in 20 mL of lysis buffer. Resuspended pellet was sonicated at 70% amplitude for 4 min. and then ultracentrifuged (35,000rpm, 4°C, 45 min.). The supernatant (load) was run through a column containing Ni^{2+}-NTA (resin) beads twice. 15 mL of wash buffer #1 was then run through the column and collected followed by 15 mL of wash buffer #2. Finally, 5 mL of the elution buffer was run through and collected in 100 µL aliquots.

SDS-PAGE Stacking Gel

0.5M Tris-HCl (pH 6.8)	1.25 µL
10% SDS	50 µL
30% Acrylamide/ Bis- acrylamide	0.65 mL
10% APS	25 µL
TEMED	5 µL
ddH_2O	3.05 mL

SDS-PAGE Separating Gel

1.5M Tris-HCl (pH 6.8)	2.5 mL
10% SDS	100 µL
30% Acrylamide/ Bis- acrylamide	3.52 mL
10% APS	50 µL
TEMED	5 µL
ddH_2O	3.83 mL

6X Laemmlli Loading Buffer

SDS	1.2 g
Bromophenol blue	6 mg
100% Glycerol	4.7 mL
0.5M Tris-HCl (pH 6.8)	1.2 mL
DTT	0.93 g
ddH_2O	2.1 mL

10X Laemmlli Running Buffer

Glycine	144 g L^{-1}
Tris Base	30.3 g L^{-1}
SDS	10 g L^{-1}

Coomassie Blue Stain

Methanol	400 mL L^{-1}
Acetic acid	100 mL L^{-1}
Coomassie blue	1 g L^{-1}

Eluted samples were then prepped by mixing 5 µL of sample with 25 µL of Laemmlli loading buffer and heated at 80°C-90°C. Samples were then loaded into an SDS-PAGE gel and ran with 1X Laemmlli running buffer. Gels were then stained with Coomassie and destained with distilled H_2O.

Pull-down Assay

Eluted 6X his-tagged protein samples were pooled together and diluted to a 20mM imidazole concentration using lysis buffer. Diluted samples were run through a column containing Ni^{2+}-NTA (resin) beads twice **(Fig. 3)**. 15 mL of wash buffer #1 was run through the column four times. A 500 mL pellet of PES13 (GpsB overexpression strain in SH1000) was

resuspended in 10 mL of lysis buffer and placed in a bead beater for 4 min. Lysed *S. aureus* cells were spun down at 10,000 rpm for 10 min. *S. aureus* lysate was then run through the Ni-column twice **(Fig. 3)**. 15 mL of wash buffer #1 was then run through. Lastly, 5 mL of the elution buffer was run through and collected in 100 µL aliquots **(Fig. 3)**. Samples were prepped, run in an SDS-PAGE gel, and silver stained using the protocol provided in the Thermo Fisher Pierce silver stain kit.

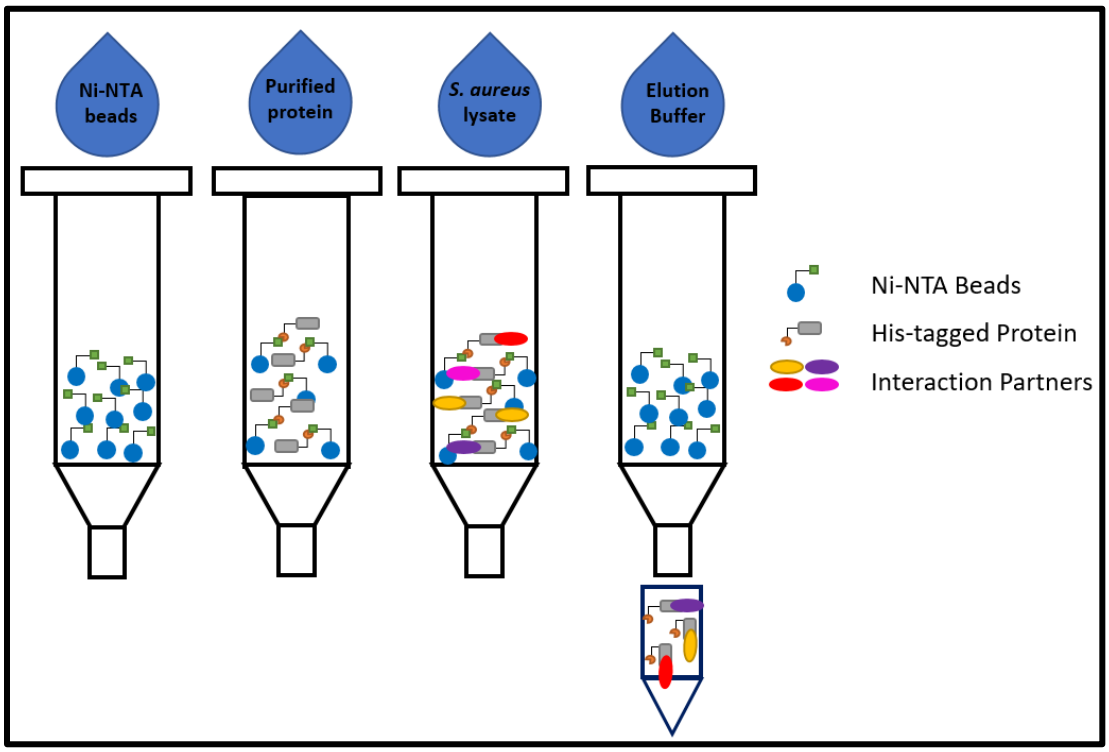

Figure 3- Pull-down Assay

Mass Spectrometry

Silver stained gels from pull-down assay were placed on glass and bands were excised from gels using a clean razor blade. Each lane was divided into three sections and each section was minced with a razor blade and placed into tubes. Minced pieces were destained in 50:50 200 mM sodium thiosulfate:60 mM potassium ferricyanide for no longer than 5 min. They were then washed with 100mM ammonium bicarbonate (ABC): acetonitrile (ACN) three times; vortexing for 10 min between washes. Gel pieces then covered in ACN and vortexed for 5 min.

ACN was removed and gel pieces were covered in 100mM ABC and vortexed for 5 min. 50:50 ACN:ABC was added to minced pieces and vortexed for 15 min. Samples were then placed in speedvac for 5 min.

Gel pieces rehydrated in 50mM dithiothreitol (DTT) for 30 min at 55°C. Samples cooled to room temperature and then covered in 100mM iodoacetamide (IAA) for 30 min. in the dark. Gel pieces washed three times for 15 min with gentle vortexing in 50:50 ACN:ABC. Speedvac samples for 5 min, then place on ice for 5 min. Lyophilized trypsin added and samples placed on ice for 30 min. Samples then incubated overnight at 37°C. Supernatant placed in new centrifuge tubes. Gel pieces then washed twice in 50:50 ACN: H_2O:0.1% formic acid. Samples placed in speedvac until completely dry. Samples then prepped for mass spectrometer by proteomics facility manager (Dr. Dale Chaput) and run in either the LTQ-OrbiXL or Q Exactive Plus with quality control samples and blanks. Raw data run against *S. aureus* proteome (NCTC 8325) and *E. coli* proteome (K12).

Western Blot

SM Buffer

0.5M Sucrose	171.2 g L^{-1}
20mM $MgCl_2$	1.9 g L^{-1}
10mM KH_2PO_4 (pH 6.5)	1.4 g L^{-1}
0.1 mg/mL Lysozyme	

10X Transfer Buffer

Glycine	144 g L^{-1}
Tris base	30.3 g L^{-1}
SDS	10 g L^{-1}

1X Transfer Buffer

10X Transfer buffer	100 mL L^{-1}
Methanol	200 mL L^{-1}
ddH_2O	700 mL L^{-1}

20X Washing Solution

1M Tris-HCl (pH 7.4)	200 mL L^{-1}
NaCl	180 g L^{-1}
Tween 20	10 mL L^{-1}
Fill to 1 L with ddH_2O	

Blocking Solution

20X Washing solution	50 mL L^{-1}
Milk powder	50 g L^{-1}
Fill to 1 L with ddH_2O	

2 mL cultures grown to OD_{600}= 0.5. Cultures grown with and without inducer for 3 hr. 2 mL pellets resuspended in SM buffer and incubated for 30 min at 37°C (*B. subtilis* ad *E. coli*). *S. aureus* samples placed in bead beater for 3 min. samples were then prepared by mixing 5 µL of sample with 25 µL of Laemmlli loading buffer and heated at 80°C-90°C. Samples then run in SDS-PAGE gel with 1X Laemmlli running buffer. Protein transferred to membrane using Thermo Fisher Mini Blot Module. Sponges, filter papers, and membrane soaked in 1X transfer buffer before being placed in apparatus. Transfer run at 10 V for 1 hr. Transfer apparatus disassembled and membrane placed in blocking solution for 1 hr. (or overnight). Primary antibody diluted 1:10,000 in 2 mL of blocking solution. Membrane left in primary antibody for 1 hr. (or overnight). Membrane then washed three times in blocking solution for 10 min. Secondary antibody (horseradish peroxidase or AP conjugated) diluted 1:3,000 in blocking

solution. Membrane left in secondary antibody for 1 hr. and then washed with blocking solution three times for 10 min.

Membrane placed in 50:50 mixture of Thermo Fisher SuperSignal West Pico Chemiluminescent substrate if horseradish peroxidase secondary antibody was used. Membrane placed in substrate for 10 min and then imaged.

Alkaline Phosphate Buffer

1M Tris-HCl (pH 9.5)	5 mL
5M NaCl	1 mL
0.1M $MgCl_2$	2.5 mL
ddH_2O	41.5 mL

Membrane placed in 10 mL alkaline phosphate buffer with 66 µL NBT and 33 µL BCIP for 30 min. Developing solution replaced with ddH_2O and imaged.

Microscopy

Overnight culture diluted 1:20 into fresh media containing appropriate antibiotic. Cultures grown with or without inducer for 2-4 hr. 500 µL sample was spun down and resuspended in ~100 µL media containing 1 µg/mL of fluorescent dye FM4-64 (membrane) and/or 2 µg/mL of DAPI (DNA). 5 µL was placed on a glass bottom dish (Mattek) and covered with a 1% agarose pad made using ddH_2O. Cells viewed using a DeltaVision Elite microscope (Applied Precision/GE Healthcare) equipped with a Photometrics CoolSnap HQ^2 camera. Seventeen planes were acquired and the images were deconvolved using SoftWorx software.

Suppressor Screening

B. subtilis strain overproducing *S. aureus* GpsB (GG8) tagged with green fluorescence protein (GFP) was streaked out for single colony isolation on LBA containing the appropriate

antibiotic and grown overnight at 37°C. LBA plate containing 1 mM Isopropyl β-D-1-thiogalactopyranoside (IPTG) was divided into six sections **(Fig. 4)**. WT *B. subtilis* (PY79) was streaked onto one section and colonies from the overnight plate containing *S. aureus* GpsB-GFP were streaked onto the other five sections and grown overnight at 37°C **(Fig. 4)**. PY79 should form a lawn and GpsB-GFP will have either no growth or a few colonies **(Fig. 4)**. A colony from each of the sections streaked with GpsB-GFP that had growth was streaked onto fresh LBA containing the appropriate antibiotic and grown overnight at 37°C. Colonies were then screened for GFP expression using fluorescence microscopy. Suppressor screening was continued with colonies expressing GFP. Chromosomal DNA was extracted from GFP-expressing colonies and transformed into PY79 **(Fig. 4)**. A fresh LBA plate containing 1 mM IPTG was again divided into sections. PY79 was streaked onto one section and one colony from each set of PY79 transformations was streaked in the other sections and grown overnight at 37°C **(Fig. 4)**. If growth is restored on the LBA + IPTG plate, there was a possible intragenic suppressor. If growth is not restored on the LBA + IPTG plate, there are possible extragenic suppressors.

Chromosomal DNA extracted from possible intragenic suppressors, region amplified via PCR and sent out for sequencing **(Fig. 4)**. For possible extragenic suppressors, original glycerol stock (before PY79 transformation) transformed with chromosomal DNA from KR168 (carries catR) **(Fig. 4)**. catR suppressor strain transformed with chromosomal DNA from GpsB-GFP *B. subtllis* strain and screened for spectinomycin resistance. Chromosomal DNA then extracted using Promega Wizard Genomic DNA Purification Kit and sent out for whole genome sequencing **(Fig. 4)**.

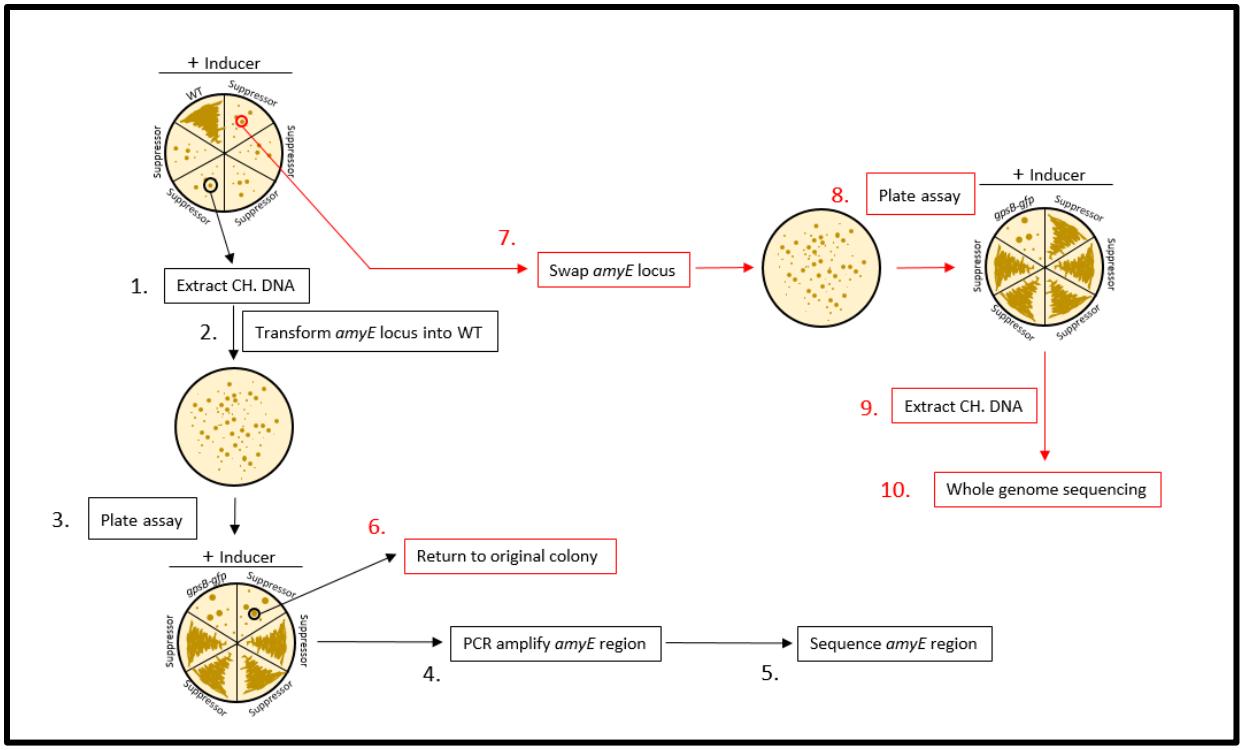

Figure 4- Suppressor Screening
Steps 1-3 followed for possible intragenic and extragenic suppressors. Steps 4-5 (black) followed for intragenic suppressors and steps 6-10 (red) followed for extragenic suppressors.

Primers

Table 2- Primer List

Primer	Oligo Sequence	Description	Cut Site
oP24	5'-GCCGCATGCTTATTTGTATAGTTCATCCATGCC-3'	*gfp* 3'	SphI
oP36	5'-AAAAAGCTTACATAAGGAGGAACTACTATGTCAGATGTTTCA TTGAAATTATCAGCA-3'	*gpsB*^{Sa} 5'	HindIII
oP37	5'-AAAGCTAGCTTTACCAAATACAGCTTTTTCTAAGTTTGA-3'	*gpsB*^{Sa} 3'	NheI
oP38	5'-AAAGCATGCTTATTTACCAAATACAGCTTTTTCTAAGTTTGA-3'	*gpsB*^{Sa} 3'	SphI
oP46	5'- AAAGCTAGC ATGAGTAAAGGAGAAGAACTTTTC-3'	*gfp* 5'	NheI
oP100	5'-AAAGTCGACACATAAGGAGGAACTACTATGCTTGCTGATA AAGTAAAGCTTTCTGCG-3'	*gpsB*^{Bs} 5'	SalI
oP101	5'-5AAAGCTAGCATCATAAAGCTTGCTGCCAAAAACGTG-3'	*gpsB*^{Bs} 3'	NheI
oP102	5'-AAAGCTAGCTCAATCATAAAGCTTGCTGCCAAAAACGTG-3'	*gpsB*^{Bs} 3'	NheI

oP128	5-CCCTCTAGAAATAATTTTGTTTAACTTTAAGAAGGAGATATAC CATGTCAGATGTTTCATTGAAATTATCAGC-3'	*gpsB*^{Sa} 5'	XbaI
oP129	5'-AAAGGATCCTTAATGATGATGATGATGATGTTTACCAAATA CAGC-3'	*gpsB*$^{Sa\text{-}his}$ 5'	BamHI
oP187	5'-AAAGAATTCTGCATCTACTTCTTCTCTTCTATAGCCACGAGCC ATCG-3'	*gpsB*^{antisense} 5'	EcoRI
oP188	5'-AAAGGATCCGAGGTGGAAAAAATGTCAGATGTTTCATTGAA ATTATCAGC-3'	*gpsB*^{antisense} 3'	BamHI
oP195	5'-AAAGGATCCTCAATCATAAAGCTTGCTGCCAAAAACGTG-3'	*gpsB*^{Bs} 3'	BamHI
oP265	5'-AAAGGATCCTTATGGAGGTGAATATATGTCAGATGTTTCA TTGAAATTATCAGCA-3'	*gpsB*^{Sa} 5'	BamHI
oP266	5'-AATAAGAATTCTTATTTACCAAATACAGCTTTTTCTAAGTTT GAAATACG-3'	*gpsB*^{Sa} 3'	EcoRI
oP267	5'-AATAAGGATCCTTATGGAGGTGAATATATGAGTAA AGG AG AAGAACTTTTC-3'	*gfp* 5'	BamHI
oP268	5'-AATAAGAATTCTTATTTGTATAGTTCATCCATGCC-3'	*gfp* 3'	EcoRI

Strain Construction

B. subtilis strains are isogenic derivatives of PY79 [49]. *S. aureus* strains are isogenic derivatives of SH1000 [50]. In *B. subtilis, gpsB* and *gpsB-GFP* were amplified using PCR. The PCR fragment was then digested using HindIII at the 5' end and NheI at the 3' end. Fragment was then inserted into the 5' HindIII and 3' NheI restriction sites in pDR111 (D. Rudner). At this site, it is placed under the control of an isopropyl β-D-1 thiogalactopyranoside (IPTG) – inducible promoter ($P_{hyperspank}$). These plasmids integrated into the *amyE* locus in the *B. subtilis* chromosome. All knockout mutants were ordered from the Bacillus Genetic Stock Center (BGSC) and were cloned into an IPTG-inducible GpsB overproduction strain (GG7). All phosphorylation site mutants were ordered as Gene blocks from Integrated DNA Technologies with amino acids 89-91 in GpsB^{Sa} mutated to alanine (A) or glutamic acid (E). Gene blocks were amplified using PCR, digested using HindIII at the 5' end and NheI at the 3' end, and inserted into pDR111.

S. aureus strains were constructed by amplifying *gpsB* or *gpsB*-GFP with PCR. For insertion into pCL15, the amplified region was cloned into the 5' HindIII and 3' SphI restriction sites downstream an IPTG-inducible promoter (P_{spac}). For insertion into pEPSA5, the amplified region was cloned into the 5' EcoRI and 3' BamHI downstream a xylose-inducible promoter. Finally, for insertion into pJB67, the amplified region was inserted into either the 5' BamHI and 3' EcoRI or 5' SalI and 3' BamHI restriction sites downstream a cadmium-inducible promoter. Plasmids were first introduced into the *S. aureus* strain RN4220 and then transduced into SH1000.

Table 3- Strains Used in Thesis

Species	Strain	Genotype	Reference
E. coli	PE401	P_{IPTG}-*gpsB*$^{Sa\text{-}his}$ kan	
B. subtilis	PY79	Wild Type	49
B. subtilis	GG7	*amyE::*$P_{hyperspank}$-*gpsB*^{Sa} spec	
B. subtilis	GG8	*amyE::*$P_{hyperspank}$-*gpsB*^{Sa}-*gfp* spec	
B. subtilis	GG9	*amyE::*$P_{hyperspank}$-*gpsB*^{Sa} spec; *ftsAZ::ftsAZ-gfp* erm	51
B. subtilis	GG18	*amyE::*$P_{hyperspank}$-*gpsB*^{Bs} spec	
B. subtilis	GG19	*amyE::*$P_{hyperspank}$-*gpsB*^{Bs}-*gfp* spec	
B. subtilis	PE377	*amyE::*$P_{hyperspank}$-*gpsB*$^{Sa\text{-}LEE}$-*gfp* spec	
B. subtilis	PE448	*amyE::*$P_{hyperspank}$-*gpsB*$^{Sa\text{-}L35S}$-*gfp* spec	
B. subtilis	CS89	*amyE::*$P_{hyperspank}$-*gpsB*$^{Sa\text{-}D41N}$-*gfp* spec	
B. subtilis	CS90	*amyE::*$P_{hyperspank}$-*gpsB*$^{Sa\text{-}E67\_L69del}$ -*gfp* spec	
B. subtilis	CS91	*amyE::*$P_{hyperspank}$-*gpsB*$^{Sa\text{-}R72H}$-*gfp* spec	
B. subtilis	CS92	*amyE::*$P_{hyperspank}$-*gpsB*$^{Sa\text{-}Y14F}$-*gfp* spec	
B. subtilis	CS93	*amyE::*$P_{hyperspank}$-*gpsB*$^{Sa\text{-}D41G}$-*gfp* spec	
B. subtilis	GG35	*amyE::*$P_{hyperspank}$-*gpsB*^{Sa} spec; *ezrA*::erm	

B. subtilis	CS94	*amyE::*$P_{hyperspank}$-*gpsB*^{Sa} spec; *divIVA*::erm	
B. subtilis	CS24	*amyE::*$P_{hyperspank}$-*gpsB*^{Sa} spec; *prkC*::erm	
B. subtilis	CS26	*amyE::*$P_{hyperspank}$-*gpsB*^{Sa} spec; *ponA*::erm	
B. subtilis	CS40	*amyE::*$P_{hyperspank}$-*gpsB*^{Sa} spec; *gpsB*^{Bs}::tet	
B. subtilis	CS9	*amyE::*$P_{hyperspank}$-*gpsB*$^{Sa\text{-}T\text{->}E}$ spec	
B. subtilis	CS10	*amyE::*$P_{hyperspank}$-*gpsB*$^{Sa\text{-}T\text{->}E}$-*gfp* spec	
B. subtilis	CS11	*amyE::*$P_{hyperspank}$-*gpsB*$^{Sa\text{-}T\text{->}A}$ spec	
B. subtilis	CS12	*amyE::*$P_{hyperspank}$-*gpsB*$^{Sa\text{-}T\text{->}A}$-*gfp* spec	
S. aureus	SH1000	Wild Type	50
S. aureus	PES13	pCL15 backbone; P_{spac}-*gpsB*^{Sa} chlor	
S. aureus	PES6	pCL15 backbone; P_{spac}-*gpsB*^{Sa}-*gfp* chlor	
S. aureus	GGS8	pEPSA5 backbone; P_{xylose}-*gpsB*$^{Sa\text{-}antisense}$ chlor	
S. aureus	PES5	pCL15 empty vector	
S. aureus	PES8	pCL15 backbone; P_{spac}-*gpsB*$^{Sa\text{-}L35S}$-*gfp* chlor	
S. aureus	CS95	pCL15 backbone; P_{spac}-*gpsB*^{Bs} chlor	
S. aureus	CS57	pJB67 backbone; P_{Cd}-*gfp* erm	
S. aureus	CS58	pJB67 backbone; P_{Cd}- *gpsB*$^{Sa\text{-}T\text{->}A}$ erm	
S. aureus	CS59	pJB67 backbone; P_{Cd}- *gpsB*$^{Sa\text{-}T\text{->}A}$-*gfp* erm	
S. aureus	CS61	pJB67 backbone; P_{Cd}- *gpsB*$^{Sa\text{-}T\text{->}E}$ erm	
S. aureus	CS63	pJB67 backbone; P_{Cd}- *gpsB*$^{Sa\text{-}T\text{->}E}$-*gfp* erm	
S. aureus	CS72	pJB67 backbone; P_{Cd}- *gpsB*^{Sa} erm	
S. aureus	CS74	pJB67 backbone; P_{Cd}- *gpsB*^{Sa}-*gfp* erm	

RESULTS

Overexpression of *S. aureus* GpsB is Toxic in *B. subtilis*

To determine if *Staphylococcal* GpsB ($GpsB^{Sa}$) acts in a manner similar to that of the *B. subtilis* GpsB ortholog ($GpsB^{Bs}$), $gpsB^{Sa}$ was cloned into *B. subtilis* under an Isopropyl β-D-1-thiogalactopyranoside (IPTG) inducible promoter and integrated into an ectopic locus in the *B. subtilis* chromosome. Without inducer, these cells exhibited no observable phenotype when plated on nutrient rich media (LBA). However, in the presence of 1 mM IPTG, WT *B. subtilis* cells (PY79) containing $gpsB^{Sa}$ or $gpsB^{Sa}$ -GFP exhibited a severe growth impairment **(Fig. 5)**. *B. subtilis* strains expressing $gpsB^{Bs}$ or $gpsB^{Bs}$-GFP under the control of an IPTG-inducible promoter did not have any observable growth defects **(Fig. 5)**. This suggests that the overexpression of $gpsB^{Sa}$ in *B. subtilis* is toxic, while $gpsB^{Bs}$ overexpression is not.

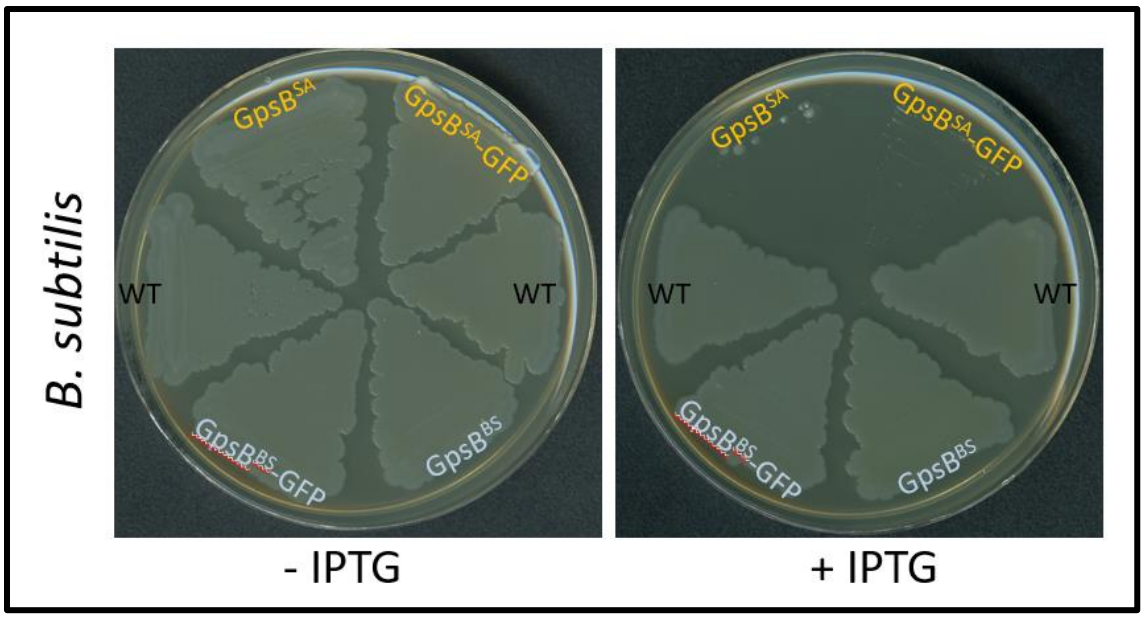

Figure 5- Overexpression of *S. aureus gpsB* Impairs Growth
LBA plates streaked with WT *B. subtilis* (PY79), or PY79 harboring an IPTG-inducible copy of *gpsB*^{Sa} (GG7), *gpsB*^{Sa} -GFP (GG8), *gpsB*^{Bs} (GG18) or *gpsB*^{Bs}-GFP (GG19) integrated into the chromosome. Growth in the absence (left) or presence (right) of IPTG shown.

To determine the cause of the severe growth impairment, *B. subtilis* cells harboring *gpsB*^{Sa} were visualized using fluorescence microscopy **(Fig. 6)**. In the absence of IPTG, the cells were of uniform length and had division septa at midcell. The DNA was also segregating normally into each daughter cell. In the presence of 1 mM IPTG, the *B. subtilis* cells expressing *gpsB*^{Sa} displayed a filamentous phenotype, DNA did not segregate properly, and cells rarely had division septa.

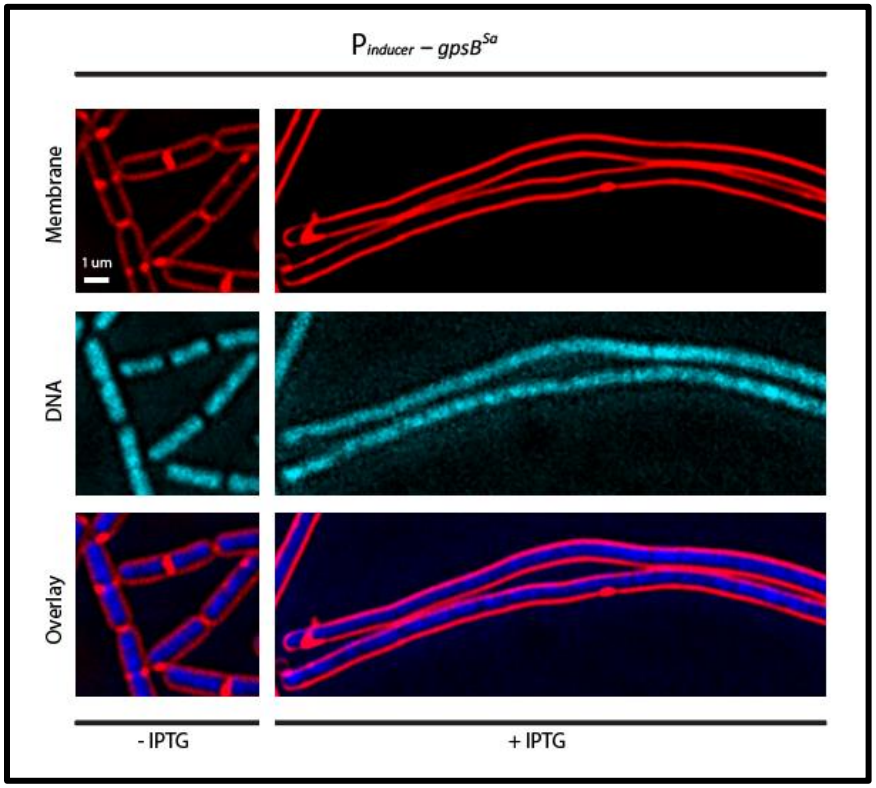

Figure 6- Overexpression of *S. aureus gpsB* in *B. subtilis* Results in Filamentation
Cell morphology of *B. subtilis* cells (GG7) in the absence of IPTG (left) and the presence of IPTG (right). Membranes stained with FM4-64 and DNA stained with DAPI.

Overexpression of *S. aureus* GpsB Disrupts Z-ring Assembly in *B. subtilis*

The filamentation observed in *B. subtilis* cells overproducing $GpsB^{Sa}$ could be due to FtsZ's inability to assemble into rings or its inability to constrict after Z-ring formation. To test this, gfp+ was fused to the *B. subtilis ftsZ* gene, integrated into the *ftsAZ* locus and expressed in a strain harboring IPTG-inducible $gpsB^{Sa}$ [51]. In the absence of IPTG, GFP-tagged FtsZ localized to midcell and cells were of uniform length **(Fig. 7)**. In the presence of IPTG, FtsZ-GFP was diffused throughout the *B. subtilis* cells overexpressing $gpsB^{Sa}$ **(Fig. 7)**. The cells also displayed a filamentous phenotype and had hardly any division septa. This indicated that the overproduction of $GpsB^{Sa}$ played a role in preventing the formation of Z-rings.

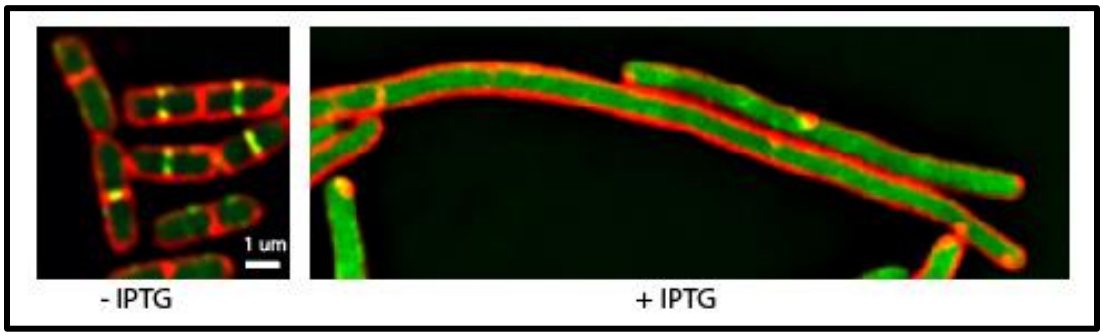

Figure 7- *S. aureus gpsB* Overexpression in *B. subtilis* Disrupts Z-Ring Assembly
Cell morphology of *B. subtilis* cells harboring an IPTG-inducible copy of $gpsB^{Sa}$ and FtsZ-GFP (GG9). Cells in the absence of IPTG (left) and the presence of IPTG (right).

$GpsB^{SA}$ Localization in *B. subtilis*

In *B. subtilis*, $GpsB^{Bs}$ shuttles between the lateral walls during elongation and the division septa upon Z-ring formation. To observe whether $GpsB^{Sa}$ follows a similar localization pattern, $gpsB^{Sa}$ -GFP was cloned into WT *B. subtilis* under the control of an IPTG-inducible promoter. In the absence of IPTG, cells were uniform in length, displayed division septa at midcell and segregated DNA properly. Upon the addition of 0.5 mM IPTG, $GpsB^{Sa}$-GFP localized to midcell and was found at cell poles **(Fig. 8)**. With the addition of 1 mM IPTG, cells became filamentous and $GpsB^{Sa}$-GFP localization no longer followed a pattern; GFP expression

was seen along the membrane and over the DNA **(Fig. 8)**. Therefore, like GpsB^{Bs}, GpsB^{Sa} localizes to midcell [21].

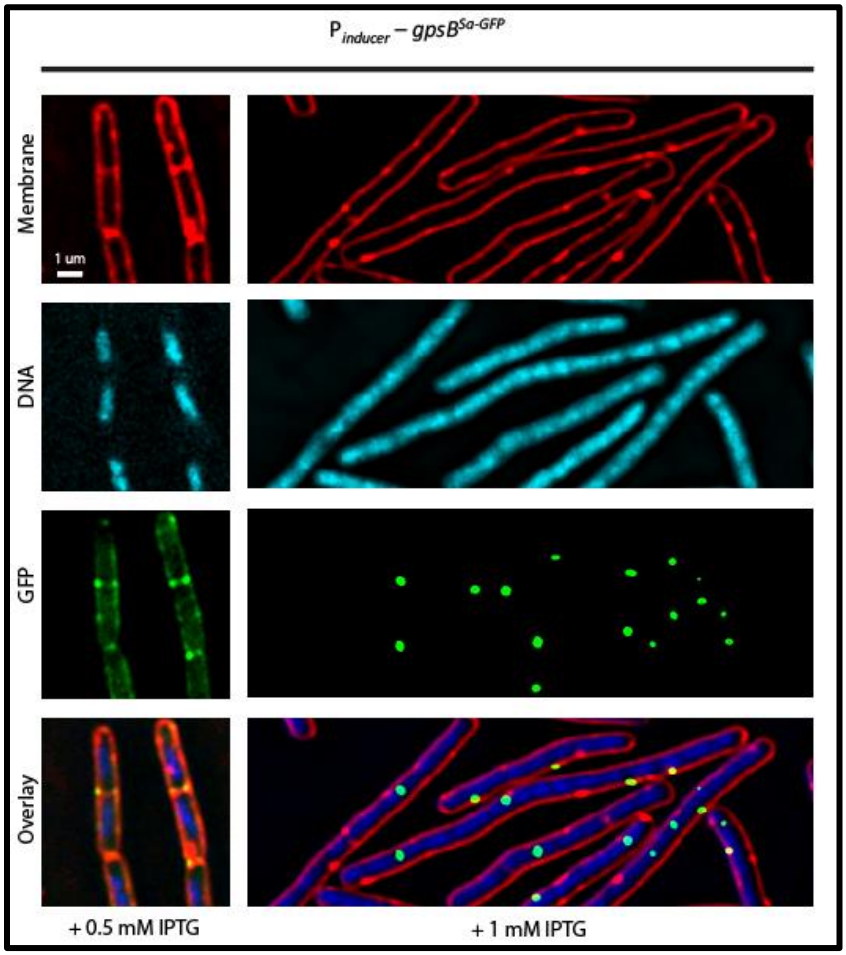

Figure 8- GpsB^{Sa} Localizes to Division Septa in *B. subtilis*
Localization of IPTG-induced *gpsB^{Sa}* -GFP (GG8) in *B. subtilis*. Cells in the presence of lower IPTG concentration (left) and higher IPTG concentration (Right).

Suppressors that Survive GpsB^{SA} Overexpression in *B. subtilis*

The overexpression of IPTG-inducible *gpsB^{Sa}* or *gpsB^{Sa}* -GFP resulted in a severe growth defect in *B. subtilis*, which was observed on the IPTG-containing plate in **Fig. 5**. While most cells overproducing GpsB^{Sa} become filamentous and do not segregate DNA properly or form division septa at midcell, we were able to isolate intragenic suppressor mutations that corrected these defects. These mutations included point mutations that resulted in the alteration

of a single amino acid: Y14F, L35S, D41N, D41G, and R72H, deletions in the nucleotide sequence that resulted in the deletion of three amino acids: E67_L69del, and insertions in the nucleotide sequence that led to the repeating of three amino acids: 68_69insLEE. The L35S, D41N, and D41G mutations altered highly conserved amino acids. *B. subtilis* cells overexpressing *gpsB*$^{Sa\text{-}L35S}$-GFP grew normally and GFP expression was diffuse throughout the cytoplasm **(Fig. 9)**. Based on the location of residue 35 in the crystal structure Rismondo *et al.* determined, the ability of the N-terminal domain to dimerize is most likely hindered in this mutant. In all the other GpsB^{Sa} mutants GFP expression was not diffuse, indicating that it was still able to form rings. In cells overexpressing *gpsB*$^{Sa\text{-}D41N}$-GFP, *gpsB*$^{Sa\text{-}D41G}$-GFP or *gpsB*$^{Sa\text{-}R72H}$-GFP, GFP expression was predominately at or near either the division septa or cell poles **(Fig. 9)**. The overexpression of *gpsB*$^{Sa\text{-}68\_69insLEE}$-GFP produced cells that grow regularly and GFP expression was at the division site, similar to WT GpsB^{Sa} **(Fig. 9)**. On the other hand, in cells overexpressing of *gpsB*$^{Sa\text{-}E67\_L69del\text{-}GFP}$-GFP, GFP expression was mostly at the cell poles **(Fig. 9)**. Finally, *gpsB*$^{Sa\text{-}Y14F}$-GFP overexpressing cells rarely had GFP expression at the division septa. Instead, GpsB localized along the lateral cell walls, near the septa and at cell poles **(Fig. 9)**. *B. subtilis* cells overproducing GpsB with any of these mutations abolished the growth toxicity, suggesting that these residues are involved in its function.

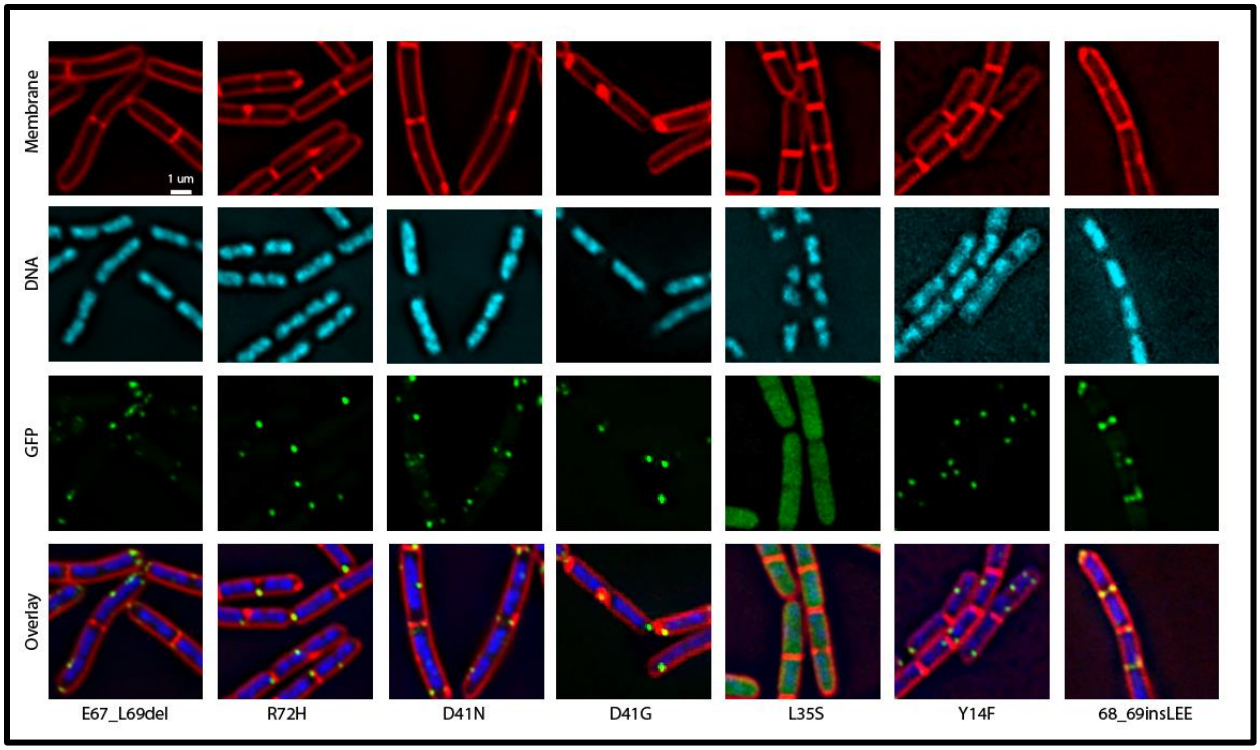

Figure 9- Suppressors Abolish Filamentous Phenotype
Localization of mutated GpsB^{Sa}. GpsB$^{Sa\text{- }E67_L69del}$-GFP (CS90) localization in column 1, GpsB$^{Sa\text{-}R72H}$-GFP (CS91) localization in column 2, GpsB$^{Sa\text{- }D41N}$-GFP (CS89) localization in column 3, GpsB$^{Sa\text{- }D41G}$-GFP (CS93) localization in column 4, GpsB$^{Sa\text{- }L35S}$-GFP (PE448) localization in column 5, GpsB$^{Sa\text{- }Y14F}$-GFP (CS92) localization in column 6, and GpsB$^{Sa\text{- }68_69insLEE}$-GFP (PE377) localization in column 7.

Deletion of Known Interaction Partners does not Prevent Filamentation

Studies in *S. pneumoniae*, *B. subtilis*, and *L. monoctyogenes* have found that in addition to interacting with itself, GpsB interacts with EzrA, DivIVA, PrkC, and PBPs [21, 22, 28, 39]. We wanted to determine if the absence of these partners would abrogate or lessen the filamentation seen in GpsB^{Sa} overproduction in *B. subtilis*. *ΔprkC*, *ΔponA* (codes for PBP1)*, ΔezrA, ΔdivIVA,* and *ΔgpsB^{Bs}* knockout mutants from the Bacillus Genetic Stock Center (BGSC) were cloned into a IPTG-inducible GpsB^{Sa} overproduction strain. In the absence of IPTG, *ΔprkC*, *ΔezrA,* and *ΔgpsB^{Bs}* did not exhibit a discernable phenotype when grown in nutrient rich LB **(Fig. 10)**. *ΔponA* cells were thinner than WT *B. subtilis* cells and *ΔdivIVA* cells were more elongated that WT *B. subtilis* without inducer **(Fig. 10)**. In the presence of 1 mM IPTG, the overexpression of

gpsB^{Sa} still resulted in a filamentous phenotype in cells lacking *ΔprkC*, *ΔponA, ΔezrA, ΔdivIVA,* or *ΔgpsB*^{Bs} **(Fig. 10).** These results indicate that these interaction partners are not necessary for GpsB^{Sa} to cause filamentation and that it is *gpsB*^{Sa} that causes the growth defect.

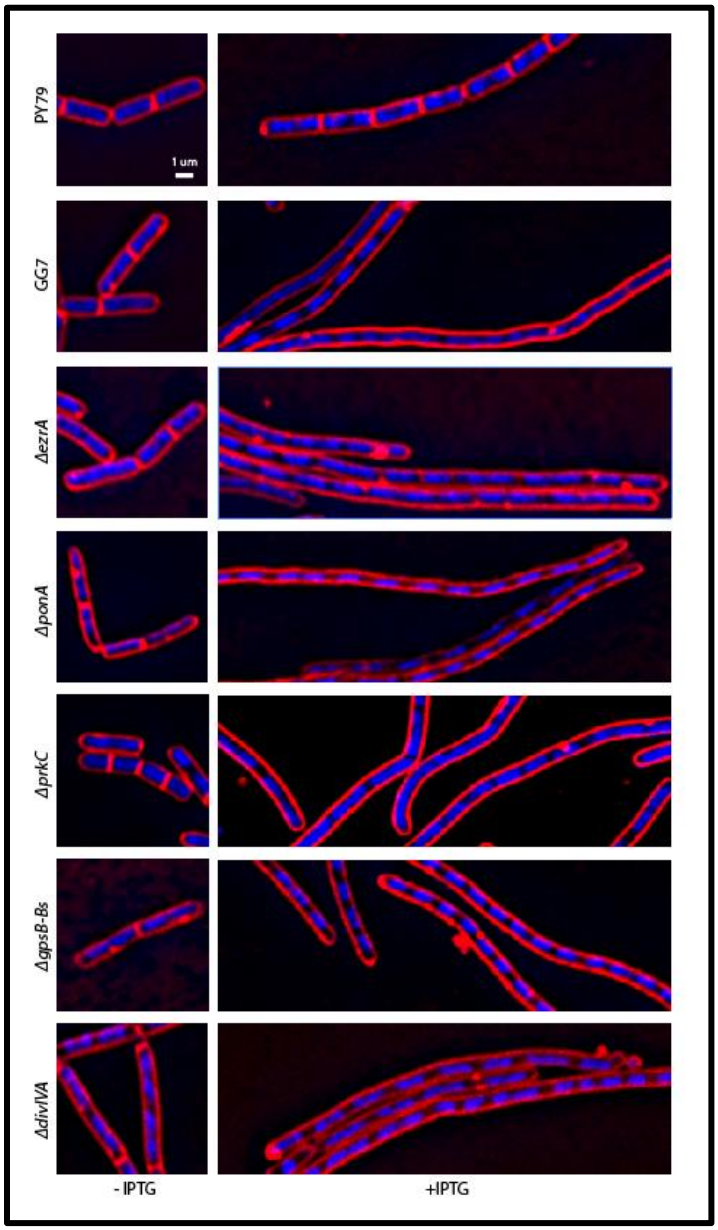

Figure 10- Absence of Interaction Partners does not Prevent Filamentation
Knockout mutants in an IPTG-inducible GpsB^{Sa} overexpression strain in the absence (left) and presence (right) of inducer.

Filamentation Present in the Absence of Possible eSTK Phosphorylation Sites

In *B. subtilis,* $GpsB^{Bs}$ is phosphorylated by the eSTK PrkC on threonine 75. The same threonine region (amino acids 89-91) is conserved in $GpsB^{Sa}$. To identify if the absence of these threonines affects cell division regulation, these residues were mutated to either alanine, which is phosphoablative, or glutamic acid, which is phosphomimetic. Gene blocks from Integrated DNA Technologies with amino acids 89-91 in $GpsB^{Sa}$ mutated to A or E were cloned into *B. subtilis* under an IPTG-inducible promoter and integrated into an ectopic locus in the *B. subtilis* chromosome. Without inducer, strains containing $gpsB^{Sa\text{-}T\text{->}A}$, $gpsB^{Sa\text{-}T\text{->}A}$-GFP, $gpsB^{Sa\text{-}T\text{->}E}$, or $gpsB^{Sa\text{-}T\text{->}E}$-GFP did not display an observable phenotype when plated on LBA **(Fig. 11)**. With inducer, all four mutant strains and the $GpsB^{SA}$ control exhibited a prominent growth defect **(Fig. 11)**. This indicated than in addition to $gpsB^{Sa}$, the overexpression of $gpsB^{Sa\text{-}T\text{->}A}$ $gpsB^{Sa\text{-}T\text{->}A}$-GFP, $gpsB^{Sa\text{-}T\text{->}E}$, or $gpsB^{Sa\text{-}T\text{->}E}$-GFP is still toxic.

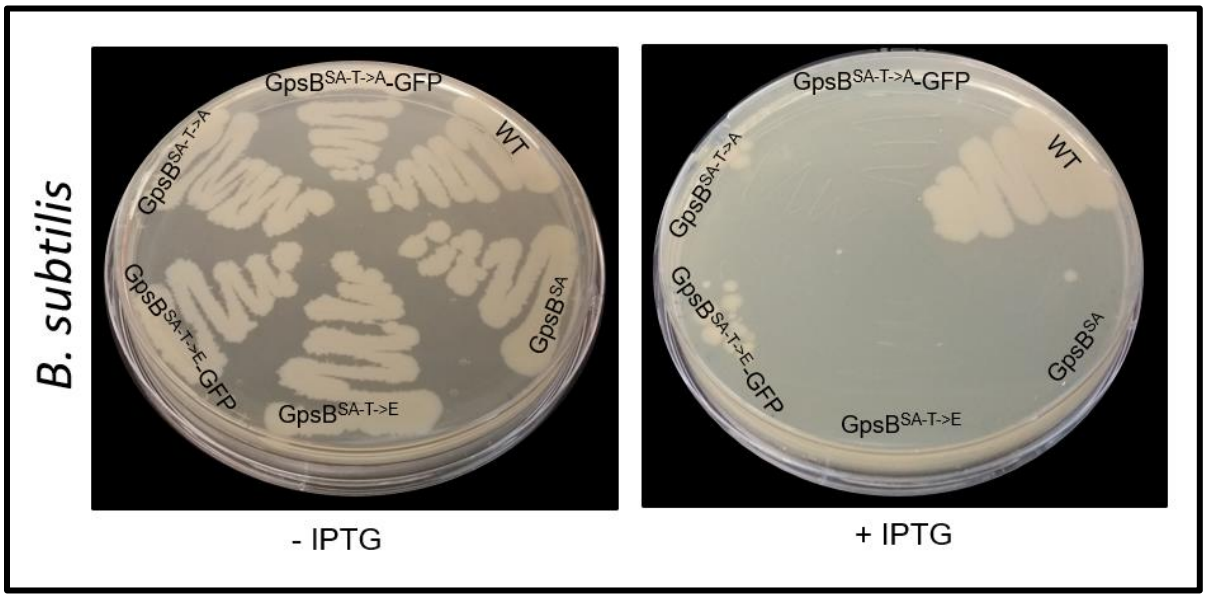

Figure 11- Overproduction of $GpsB^{Sa}$ Mutants is Toxic in *B. subtilis*
LBA plates streaked with WT *B. subtilis* (PY79), or PY79 harboring an IPTG-inducible copy of $gpsB^{Sa\text{-}T\text{->}E}$ (CS9), $gpsB^{Sa\text{-}T\text{->}E}$ -GFP (CS10), $gpsB^{Sa\text{-}T\text{->}A}$ (CS11), or $gpsB^{Sa\text{-}T\text{->}A}$ -GFP (CS12) integrated into the chromosome. Growth in the absence (left) or presence (right) of IPTG shown.

To determine if these mutants also display severe filamentation and to see if there were any changes in the localization of GpsB, GpsB$^{Sa\text{-}T\text{->}A}$, GpsB$^{Sa\text{-}T\text{->}A}$-GFP, GpsB$^{Sa\text{-}T\text{->}E}$, and GpsB$^{Sa\text{-}T\text{->}E}$-GFP were visualized using fluorescence microscopy. In the absence of inducer, GpsB$^{Sa\text{-}T\text{->}A}$ and GpsB$^{Sa\text{-}T\text{->}E}$ resembled WT cells **(Fig. 12)**. With the addition of 0.5 mM IPTG, cells were WT in size and the GFP-tagged mutant GpsB^{Sa} could localize to midcell **(Fig. 13)**. With the addition of 1 mM IPTG, both tagged and untagged mutants became filamentous **(Fig. 12 and 13)**. GpsB$^{Sa\text{-}T\text{->}A}$-GFP and GpsB$^{Sa\text{-}T\text{->}E}$-GFP localized along the membrane **(Fig. 13)**. While no changes were observed in GpsB^{Sa} localization and cells still became filamentous, the significance of possible phosphorylation of GpsB^{Sa} is not clear.

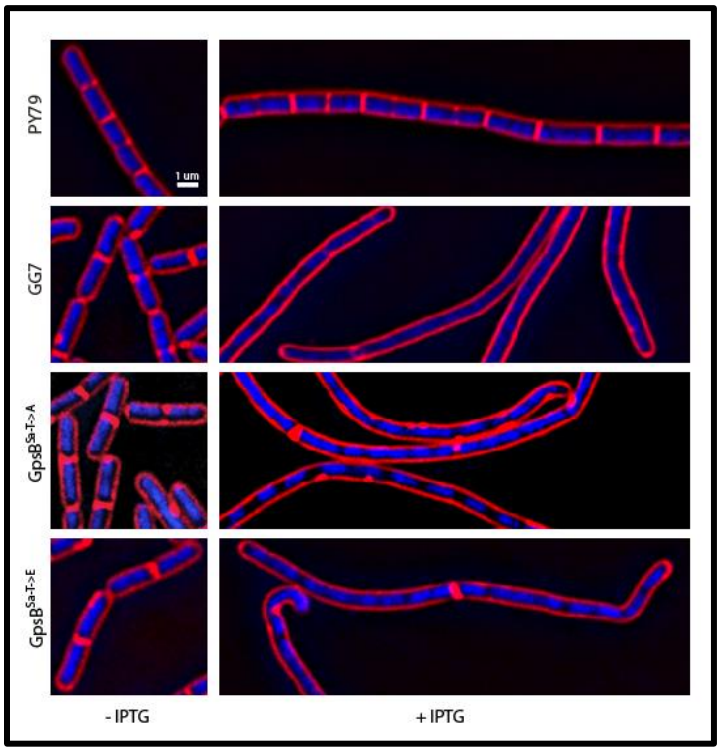

Figure 12- Filamentation Phenotype Occurs in GpsB^{Sa} Mutants in *B. subtilis*
Overexpression of IPTG-inducible inducible *gpsB$^{Sa\text{-}T\text{->}E}$* (CS9) or *gpsB$^{Sa\text{-}T\text{->}A}$* (CS11) leads to the production of filamentous cells similar to the *gpsB^{Sa}* (GG7) overexpression strain.

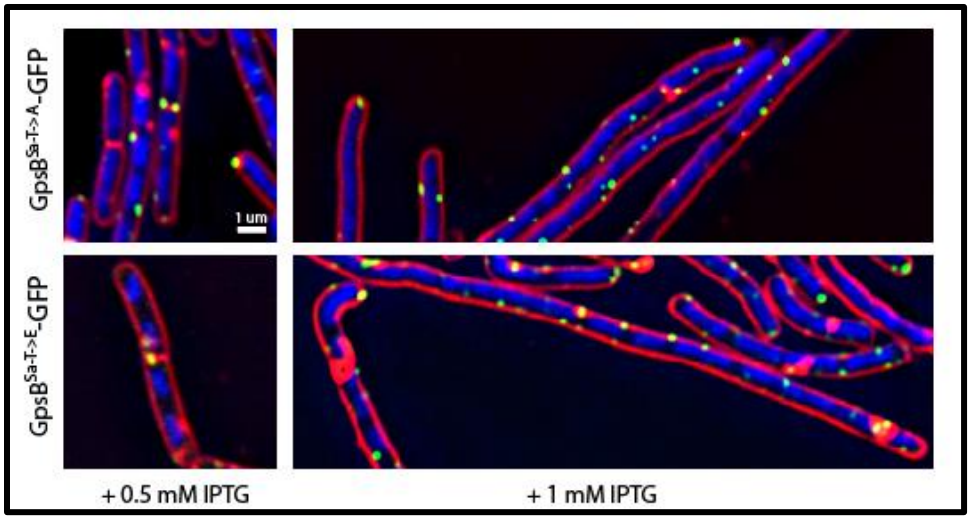

Figure 13- Mutated GpsB^{Sa} does not Disrupt Filamentation Phenotype
Localization of IPTG-induced *gpsB*$^{Sa-T->E}$ -GFP (CS10) or *gpsB*$^{Sa-T->A}$ -GFP (CS12) in *B. subtilis*. Cells in the presence of lower IPTG concentration (left) and higher IPTG concentration (Right).

Overproduction of GpsB^{Sa} is Toxic in *S. aureus*

Since GpsB^{Sa} overexpression had an effect on bacterial cell division in *B. subtilis*, we were interested in its effects in *S. aureus*. *gpsB*^{Sa} was cloned into a high copy plasmid under the control of an IPTG-inducible promoter and introduced into the WT *S. aureus* strain SH1000; this strain was then visualized using fluorescence microscopy. In the absence of IPTG, cells were approximately 1 µM in diameter, formed septa at midcell, and segregated DNA properly **(Fig. 14)**. In the presence of 1 mM IPTG, cells increased in diameter and many of the enlarged cells did not display a division septum **(Fig. 14)**. Quantification of 200 cells revealed that more than half of the cells were larger in the presence of IPTG compared to cells in the absence of IPTG.

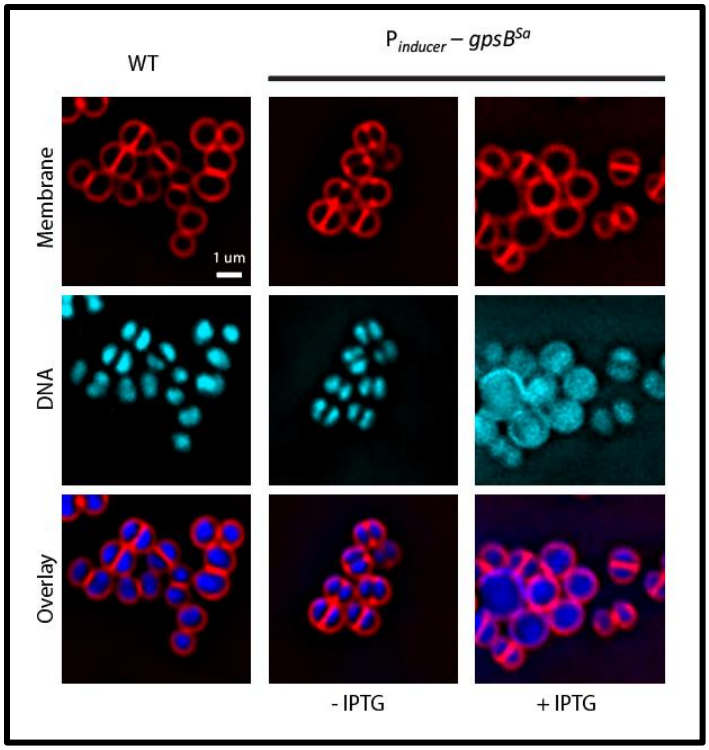

Figure 14- Overproduction of GpsB^{Sa} is Toxic in *S. aureus*
Cell morphology of *S. aureus* cells harboring an IPTG-inducible copy of *gpsB^{Sa}* (PES13) in the absence (middle) and presence (right) of IPTG.

Depletion of GpsB^{Sa} Results in Cell Lysis in *S. aureus*

The *gpsB* gene was found to be essential in *S. aureus* [47]. We were therefore unable to knockout the gene. Instead, we depleted GpsB^{Sa} through the overexpression of *gpsB^{Sa}* antisense RNA under the control of a xylose-inducible promoter in a multicopy plasmid. We examined cells using fluorescence microscopy. In the absence of xylose, cells were WT in size, segregated DNA properly, and formed division septa **(Fig. 15)**. In the presence of xylose, there was membrane debris and diffuse DAPI stain, indicative of cell lysis **(Fig. 15)**. Membrane thickening was also present. Time lapse microscopy was then performed on *gpsB^{antisense}* producing cells. At the onset of division, the daughter cells were slightly elongated and undergoing DNA separation **(Fig. 16)**. As the cycle progressed, cells improperly segregated the

replicated chromosomes to only one daughter cell; this produced anucleated cells **(Fig. 16)**.

These results are indicative of a timing defect in cell division due to the absence of GpsB^{Sa}.

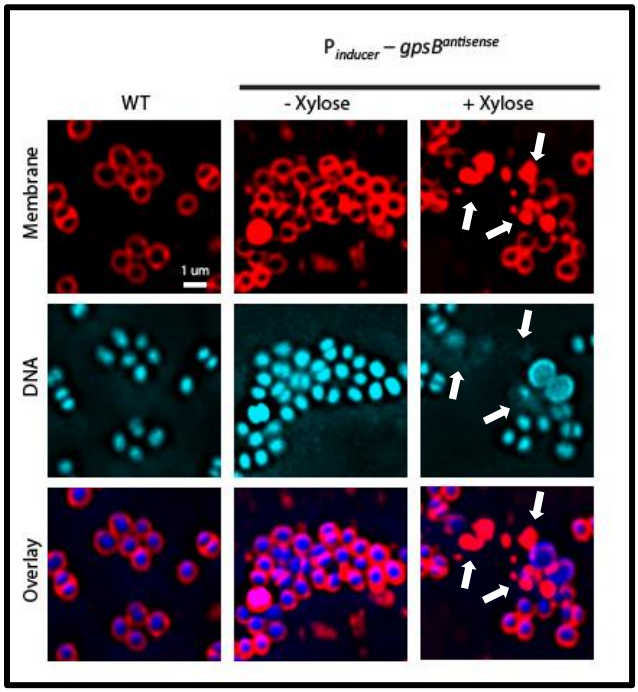

Figure 15- GpsB^{Sa} Depletion in *S. aureus*
Wild type *S. aureus* cells (SH1000) (left) or *S. aureus* containing a plasmid encoding a xylose-inducible copy of *gpsB^{antisense}* (GGS8) in the absence (middle) or presence (right) of xylose. Arrows indicate areas of cell lysis.

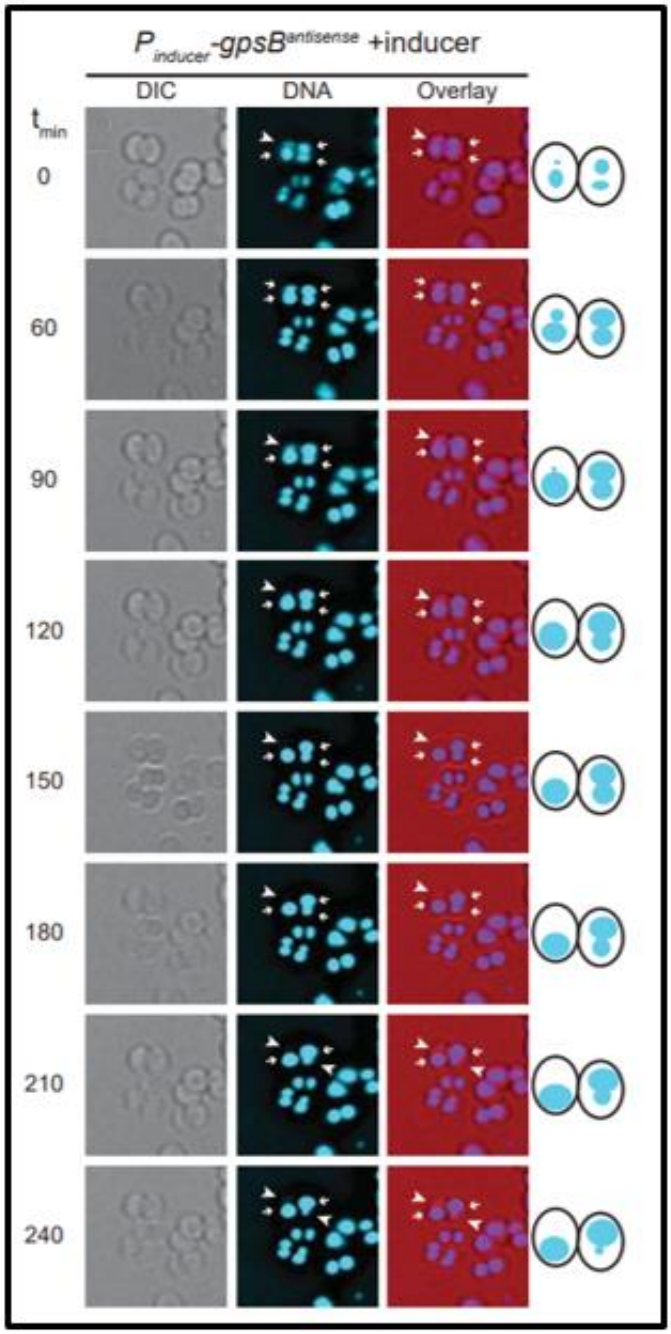

Figure 16- Improper DNA Segregation in GpsB^{Sa} Depleted Cells
Time lapse fluorescence micrographs of two dividing *S. aureus* cells overexpressing *gpsB* antisense RNA. Images taken at time intervals listed at the left. Arrowheads represent cells that DNA did not segregate into and arrows point to cells with DNA. Cells visualized using differential interference contrast (DIC) (left), chromosomes visualized using DAPI (middle), and overlay of DIC and DAPI (right).

GpsB^{Sa} Localization in *S. aureus*

To gain insight into how GpsB^{Sa} influences cell division, we observed the localization of GpsB^{Sa}-GFP in *S. aureus* using time lapse fluorescence microscopy. GpsB^{Sa}-GFP was expressed at lower levels that did not result in cell enlargement or cell division inhibition. In dividing cells, GpsB^{Sa}-GFP localized to the division septa between segregating nucleoids **(Fig. 17)**. Upon the completion of a round of division, GpsB^{Sa}-GFP redistributed to the cell periphery **(Fig. 17)**. Structured illumination microscopy (SIM) performed by our collaborators at the National Institute of Health (NIH) further revealed that in addition to localizing to midcell, GpsB^{Sa}-GFP forms a ring structure and co-constricts with the divisome **(Fig. 18)**.

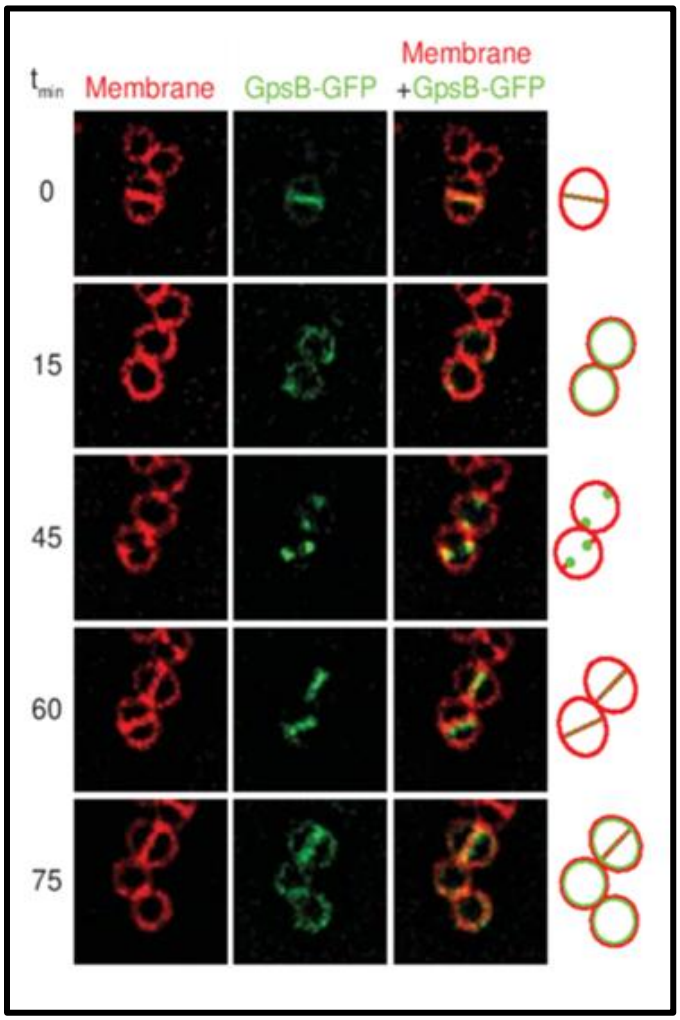

Figure 17- Redistribution of GpsB^{Sa} from Midcell to Periphery in *S. aureus* During Cell Cycle

Localization of GpsB^{Sa}-GFP (PES6) to midcell in actively dividing cells and the cell periphery in non-dividing cells. Membranes viewed using FM46-4 (left), GFP fluorescence (middle) and overlay of GFP and membrane (right).

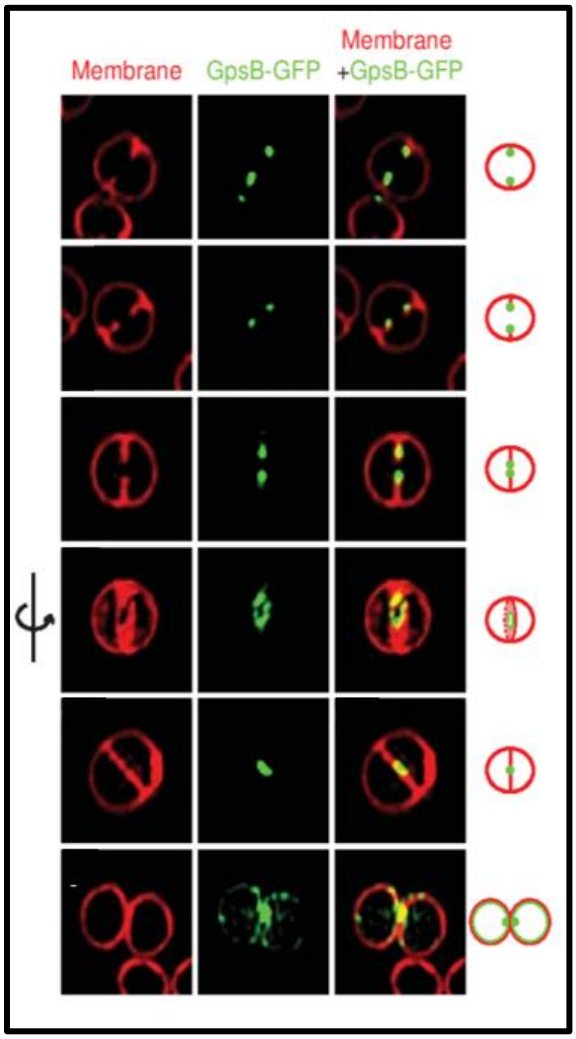

Figure 18- GpsB^{Sa}-GFP forms a Ring at Midcell

GpsB^{Sa}-GFP localization throughout the stages of division. Structured illumination microscopy was used to visualize the *S. aureus* cells.

GpsB$^{Sa\text{-}L35S}$-GFP Unable to Localize to Midcell in *S. aureus*

Of the intragenic suppressors identified, GpsB$^{Sa\text{-}L35S}$-GFP was the only one that appears to disrupt the structure of GpsB^{Sa}. Therefore, it diffused throughout the cytosol when viewed in *B. subtilis* and was unable to localize to the periphery or midcell. To see if this also occurred in *S. aureus*, *gpsB$^{Sa\text{-}L35S}$*-GFP was clone into a high copy plasmid under an IPTG-inducible promoter and transformed into WT *S. aureus*. Upon the addition of 0.5 mM IPTG, GpsB^{Sa}-GFP localized to the division septa in actively dividing cells and to the periphery in non-dividing cells **(Fig. 19)**. While GpsB$^{Sa\text{-}L35S}$-GFP remained disperse throughout the cytosol in both dividing and non-dividing cells **(Fig. 19)**. This confirmed that the highly conserved leucine is vital to how GpsB^{Sa} regulates cell division.

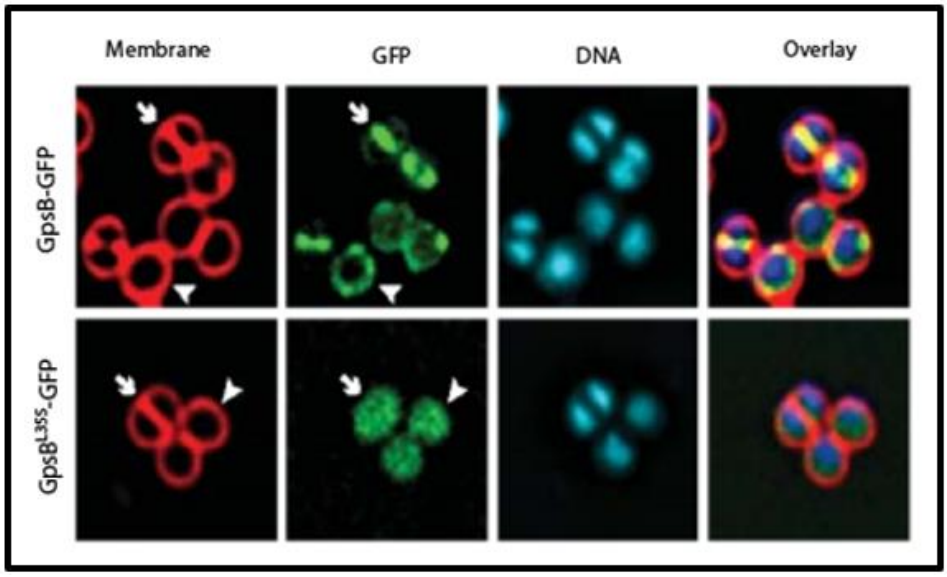

Figure 19- Localization of GpsB$^{Sa\text{-}L35S}$-GFP in *S. aureus*
Arrow shows localization of GpsB^{Sa}-GFP (PES6) in *S. aureus* (top) to midcell in actively dividing cells and to the periphery (arrowhead) in non-dividing cells. Bottom panel arrow indicates localization of GpsB$^{Sa\text{-}L35S}$-GFP in actively dividing cells versus cells that are not dividing (arrowhead).

Uncovering the Interaction Partners of GpsB^{Sa}

In *B. subtllis*, GpsB^{Bs} was reported to interact with many cell division proteins, which include PBP1 and EzrA [21]. Unlike in *B. subtilis*, *gpsB* is essential in *S. aureus*, suggesting that it is involved in non-redundant roles. To understand the pathways GpsB^{Sa} utilizes to regulate cell division, we took an unbiased approach and performed a GpsB^{Sa}-his pull-down assay as described in the methods section. We identified the proteins that were pulled down via mass spectrometry. The identified proteins are listed in **Table 4**. Of these interaction partners, PBP3 is of great interest because GpsB was found to interact with PBPs in organisms like *L. monocytogenes* and *B. subtilis*.

Table 4- GpsB^{Sa} Interaction Partners

Protein	Function
GpsB	PBP1 shuttling protein
FtnA	Iron storage protein
PBP3	Transpeptidase
McsA	Protein-arginine kinase activator
IsaA	Probable transglycosylase
RpsO	30S ribosomal protein
RplR	50S ribosomal protein
RplO	50S ribosomal protein
RpIL	50S ribosomal protein
RpmA	50S ribosomal protein
RpmF	50S ribosomal protein
Rnj1	Ribonucleases
Rnj2	Ribonucleases
AcpS	Holo-[acyl-carrier-protein] synthase

Fur	Ferric uptake regulation
Asp23	Alkaline shock protein 23
SAOUHSC_00450	Putative Orn/Lys/Arg decarboxylase
SAOUHSC_01287	Glutamine synthetase
SAOUHSC_00895	Glutamate dehydrogenase

GpsB^{Sa}-GFP Localization Upon Addition of FtsZ Inhibitor in *S. aureus*

After observing that GpsB^{Sa}-GFP localized to the septum, we wanted to determine if this localization depends on FtsZ. IPTG-inducible GpsB^{Sa}-GFP was observed using fluorescence microscopy in the presence and absence of PC190723. PC190723 is a derivative of 3-methoxybenzamide that inhibits the GTPase activity of FtsZ in *S. aureus* [52, 53]. In the presence of 1 mM IPTG, *S. aureus* strains overexpressing *gpsB^{Sa}* or *gpsB^{Sa}*-GFP were enlarged compared to WT *S. aureus* (SH1000) and GFP-tagged GpsB^{Sa} localized to midcell **(Fig. 20)**. In the presence of 1mM IPTG and 1 µg mL^{-1} PC190723, for 1 hr., SH1000 exhibited cells with septum abnormalities, GpsB^{Sa} overproducing cells were enlarged and rarely displayed division septa, and GpsB^{Sa}-GFP expressing cells became larger and GpsB^{Sa}-GFP either formed clumps or localized at or adjacent to midcell **(Fig. 20)**. GpsB^{Sa}-GFP localization was therefore changed in response to FtsZ inhibition.

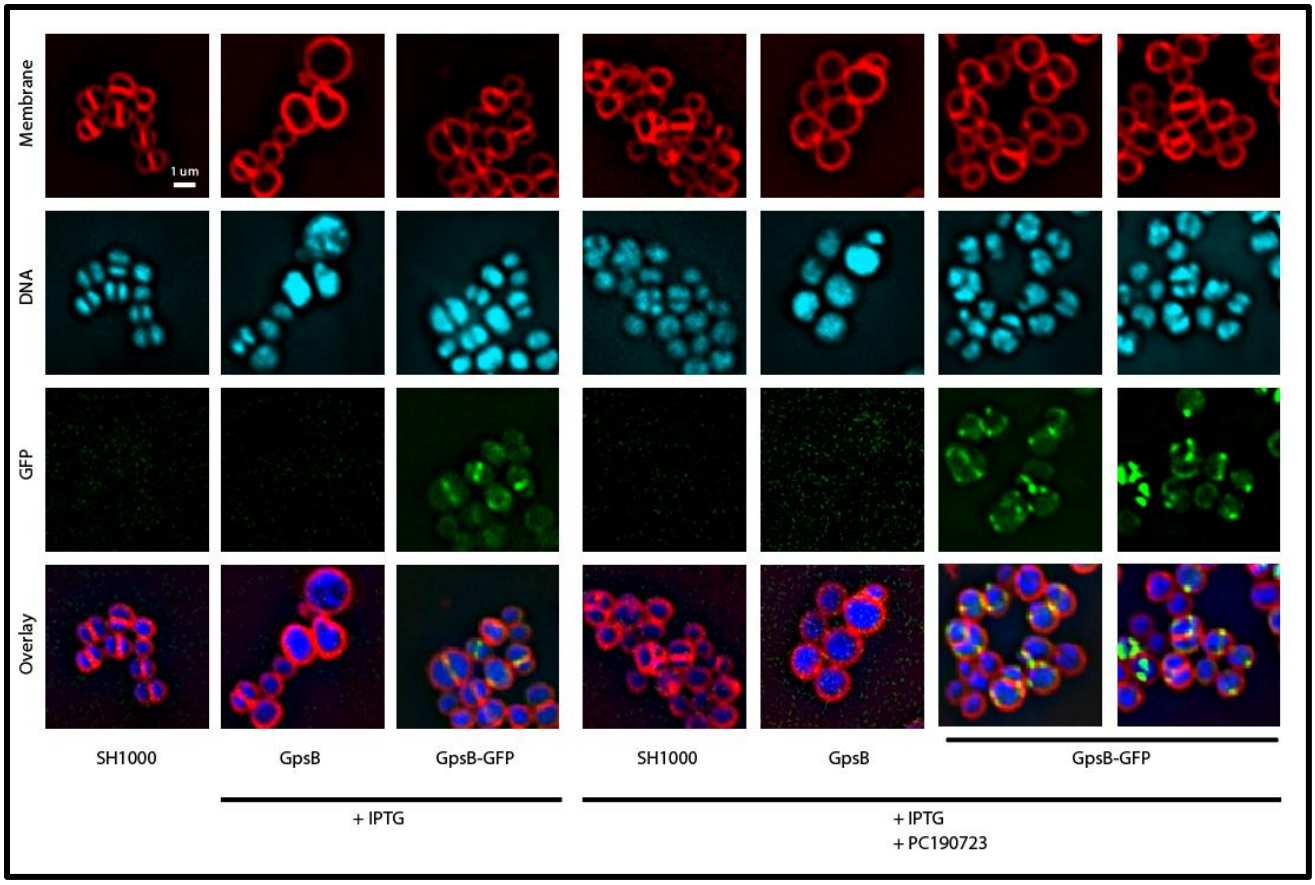

Figure 20- GpsB^{Sa}-GFP Localization Following Inhibition of FtsZ
Localization of IPTG-induced *gpsB^{Sa}* -GFP (PES6) in *S. aureus* in the absence (column 3) and presence (columns 6-7) of PC190723. Enlargement of *gpsB^{Sa}* overexpressing strain (PES13) in the absence (column 2) and presence (column 5) of PC190723. Division septa abnormalities in WT S. aureus (SH1000) following the addition of PC190723 (column 4).

Expression of Mutants in *S. aureus* does not Alter Localization

Since the overexpression of mutated threonine residues in GpsB^{Sa} did not prevent filamentation or alter localization in *B. subtilis*, we wanted to know the effect the expression of mutated GpsB^{Sa} had on cell division in *S. aureus*. We cloned *gfp*, *gpsB^{Sa}*, *gpsB$^{Sa\text{-}T\text{->}A}$*, *gpsB$^{Sa\text{-}T\text{->}E}$*-GFP, *gpsB$^{Sa\text{-}T\text{->}E}$*, or *gpsB$^{Sa\text{-}T\text{->}A}$*-GFP into the cadmium-inducible plasmid pJB67. In the presence of 12.5 µM cadmium, cell enlargement was rarely observed in cells producing GpsB^{Sa} or GpsB^{Sa}-GFP compared to strains in the pCL15 backbone **(Fig. 21)**. Enlargement of cells was also absent in cells expressing *gpsB$^{Sa\text{-}T\text{->}A}$*, *gpsB$^{Sa\text{-}T\text{->}A}$*-GFP, *gpsB$^{Sa\text{-}T\text{->}E}$*, or *gpsB$^{Sa\text{-}T\text{->}E}$*-GFP **(Fig.**

21). In the presence of 12.5 µM cadmium, GpsB^{Sa}-GFP localized to midcell and could also be see around the periphery of some cells; this was also observed in cells expressing *gpsB*$^{Sa\text{-}T\text{->}A}$-GFP or *gpsB*$^{Sa\text{-}T\text{->}E}$-GFP **(Fig. 21)**. We did not note any changes in localization pattern between mutated and non-mutated GpsB^{Sa}-GFP. Additionally, since GpsB^{Sa} and GpsB^{Sa}-GFP cells were not large compared to WT SH1000 cells, we could not draw any conclusions regarding whether the mutation to alanine or glutamate attenuated cell enlargement.

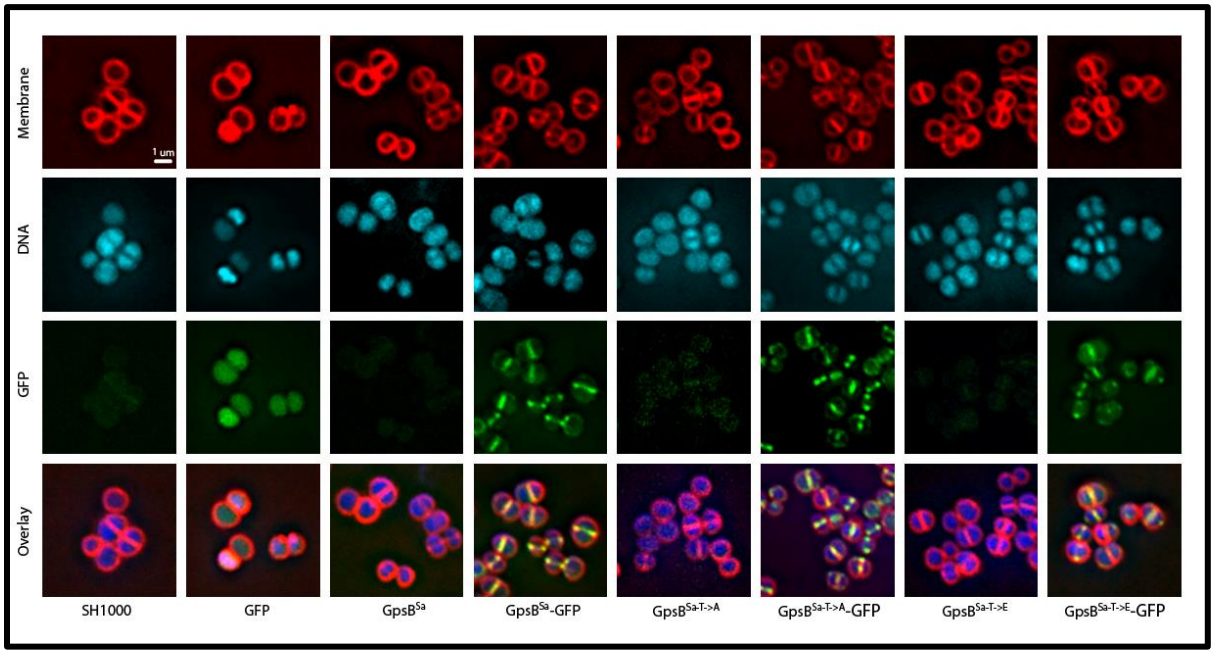

Figure 21- Localization of GpsB^{Sa} Mutants in *S. aureus*
Cell size and GpsB^{Sa} localization in pJB67 backbone. WT SH1000 (column 1) and *gfp* expressing cells (CS57) (column 2) compared to cells expressing *gpsB*^{Sa} (CS72) (column 3), *gpsB*^{Sa}-GFP (CS74) (column 4), *gpsB*$^{Sa\text{-}T\text{->}A}$ (CS58) (column 5), *gpsB*$^{Sa\text{-}T\text{->}A}$-GFP (CS59) (column 6), *gpsB*$^{Sa\text{-}T\text{->}E}$ (CS61) (column 7), and *gpsB*$^{Sa\text{-}T\text{->}E}$-GFP (CS63) (column 8).

Overexpression of GpsB^{Bs} in *S. aureus*

After observing both *B. subtilis* and *S. aureus* cells overexpressing *gpsB*^{Sa}, we wanted to know if *S. aureus* cells producing GpsB^{Bs} exhibited any division defects. To do this, we cloned *gpsB*^{Bs} into a high copy plasmid under the control of an IPTG-inducible promoter and transduced it into WT SH1000. In the absence of IPTG, cells appeared WT in size, displayed

division septa, and segregated DNA properly **(Fig. 22)**. In the presence of IPTG, cells containing the empty pCL15 vector remained WT in size, while *gpsB*^{Sa} expressing cells became enlarged and some had condensed DNA or other DNA abnormalities **(Fig. 22)**. Some *gpsB*^{Bs} expressing were larger than WT, but did not appear as large as the *gpsB*^{Sa} expressing cells **(Fig. 22)**. These results show that the increase in cell size is more severe when GpsB^{Sa} is overproduced.

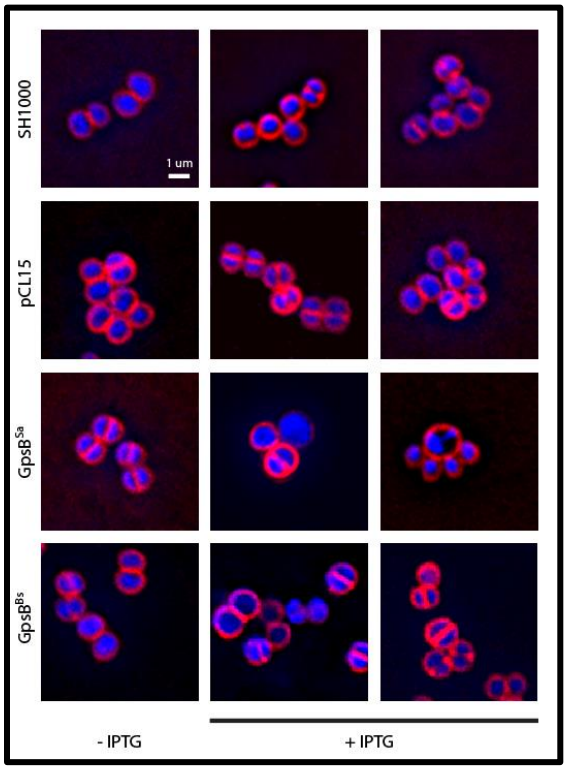

Figure 22- GpsB^{Bs} Overexpression in *S. aureus*
Overproduction of GpsB^{Sa} (PES13) and GpsB^{Bs} (CS95) in *S. aureus* compared to WT SH1000 and cells containing the pCL15 empty vector (PES5).

DISCUSSION

Cell division regulation has predominately been studied in rod-shaped model organisms, such as *E. coli* and *B. subtilis*. The mechanisms behind cell division regulation in spherical bacteria have not been characterized as well. Here we investigated the role of $GpsB^{Sa}$ during cell division in the spherical bacterium, *S. aureus*. These results indicate that $GpsB^{Sa}$ inhibits FtsZ, a core component of the division machinery. This is supported by the cell enlargement phenotype exhibited following the overexpression of $gpsB^{Sa}$; a phenotype resembling that caused by depletion of FtsZ (54). The overexpression of $gpsB^{Sa}$ in *B. subtilis* cells harboring FtsZ-GFP, further revealed that Z-ring assembly was impaired. $GpsB^{Sa}$-GFP localization was also altered upon FtsZ inhibition in *S. aureus*. Instead of localizing at midcell, $GpsB^{Sa}$-GFP was found off center to the septa or as clumps. Previous studies in *S. aureus* have shown that over time cells become enlarged following PC190723 treatment because the Z-ring cannot constrict [52]. Therefore, it is possible that $GpsB^{Sa}$-GFP is not going to the septum, and is instead remaining where FtsZ localized before its GTPase activity was hindered. These findings are interesting because the orthologs of GpsB in *L. monocytogenes*, *S. pneumoniae*, and *B. subtilis* have not been shown to interact with FtsZ. Additional evidence that $GpsB^{Sa}$ acts in a manner that differs from its orthologs is the fact that overexpression of $gpsB^{Sa}$ in *B. subtilis* results in filamentation, while overexpression of $gpsB^{Bs}$ did not result in any observable phenotype.

To further discern the mechanism(s) $GpsB^{Sa}$ utilizes to regulate cell division, we set forth to identify interaction partners using a pull-down assay. Studies in *S. pneumoniae*, *B. subtilis*, and *L. monocytogenes* have found that in addition to interacting with itself, GpsB interacts with EzrA, DivIVA, PrkC, and PBPs [21, 22, 28, 39]. The interaction between GpsB and EzrA that

occurs in *B. subtilis* was proposed to be conserved in *S. aureus*, due to GpsB^{Sa}'s delocalization upon EzrA depletion [48, 49]. However, our mass spectrometry data did not include EzrA as an interaction partner. Serine/Threonine protein kinases (STPKs) and DivIVA were also not identified in the mass spectrometry data. We did however pull-down GpsB^{Sa} and the penicillin binding protein PBP3. While no phenotypes have been associated with the inactivation of *pbp3*, a decrease in autolysis was the only effect that has been observed [55]. Further studies would need to be done to determine if PBP3 influences the overexpression phenotype observed following *gpsB^{Sa}* overexpression in *S. aureus*. Finding a link between PBP3 and GpsB^{Sa} would also show that it shares some functions observed in its orthologs.

Suppressor screening led to the identification of seven mutations that abrogated the filamentous phenotype observed in *B. subtilis* cells overexpressing *gpsB^{SA}*-GFP. Of these mutations, three (L35S, D41N, and D41G) occurred at highly conserved residues. These conserved residues are potentially involved in similar roles across species. It can also be concluded that these residues are all required for GpsB^{Sa} to function properly.

The absence of EzrA, DivIVA, and STPKs as interaction partners also provides insight into why their absence did not prevent or minimize the filamentation phenotype observed upon *gpsB^{Sa}* overexpression in *B. subtilis*. If these proteins are not involved in the mechanism GpsB^{Sa} uses to regulate cell division, then it is unlikely that their absence would correct the division defect exhibited in filamentous cells. GpsB^{Sa} may also be unable to phosphorylate or be phosphorylated by the *B. subtilis* eSTK, PrkC. Therefore, deletion of *prkC* did not prevent filamentation and mutation of possible phosphorylation sites did not alter the localization pattern observed with the *gpsB^{Sa}*-GFP expressing strain. We plan to execute similar experiments in an *S. aureus* background to further validate our observations.

Additionally, we did not observe any changes in GpsB^{Sa} localization with the mutated strains in *S. aureus*, and we did not see the cell enlargement phenotype that usually occurs in GpsB^{Sa} overproducing cells. Since cadmium is toxic to cells at high concentrations and after

prolonged periods, we used low concentrations to induce cells and only let cells grow for a couple of hours. Due to these limitations, cell may not be producing GpsB^{Sa}, GpsB$^{Sa\text{-}T\text{->}A}$, GpsB$^{Sa\text{-}T\text{->}A}$-GFP, GpsB$^{Sa\text{-}T\text{->}E}$, or GpsB$^{Sa\text{-}T\text{->}A}$-GFP at high enough levels. It is also possible that even at higher levels, there would be no changes in localization patterns or cell enlargement. Further testing is still necessary in order to make any conclusions regarding the impact these threonine residues have on GpsB^{Sa} and whether they are in fact phosphorylated by a eSTK.

Collectively, these results show that GpsB^{Sa} is essential in *S. aureus* and is involved in cell division. While more research need to be done to pinpoint the mechanism(s) GpsB^{Sa} uses to facilitate division, the observations detailed here point to FtsZ and potentially PBP3 as being involved.

FUTURE DIRECTIONS

To further explore the possible link between GpsB^{Sa} and PBP3, we would like to see if the *gpsB*^{Sa} overexpression phenotype is attenuated in a *pbpC*::tn background in *S. aureus*. We would also like to continue looking for other interaction partners using a co-immunoprecipitation assay and analyzing the protein-protein interactions through mass spectrometry.

While the crystal structures of GpsB from *B. subtilis* and *L. monocytogenes* have been solved, we are still interested in doing structural analysis of GpsB^{Sa} and the complex of GpsB^{Sa} with its interaction partners. Homology modeling, X-ray crystallography, and NMR spectroscopy are all viable options for obtaining the structure of *S. aureus* GpsB. We have new data to show that GpsB^{Sa} is interacting with FtsZ and we are interested in solving the structure of the GpsB^{Sa}-FtsZ complex to identify the amino acids involved in the interaction. Additionally, we could use fluorescently labeled proteins to monitor localization of GpsB^{Sa} with FtsZ, PBP3, and other possible interactors. We would also like to continue studying the possibility of GpsB^{Sa} phosphorylation and its effects.

Through suppressor screening, seven mutants were isolated. Thus far we have only looked at GpsB$^{Sa\text{-}L35S}$-GFP localization at lower IPTG concentrations in *S. aureus*. While the L35S mutation mimicked the diffuse cytosolic localization that was observed in *B. subtilis*, we would like to see how the other mutations impact localization and function in *S. aureus*.

Additionally, we want to show what happens to GpsB^{Sa}-GFP localization in the absence of FtsZ. While the use of PC190723 allowed us to visualize GpsB^{Sa}-GFP localization when the Z-ring was unable to constrict, FtsZ was still present and therefore GpsB^{Sa} had the ability to

localize to where FtsZ was present. We can achieve this by introducing GpsB^{Sa}-GFP into a strain in which ftsZ expression is controlled by an IPTG-inducible promoter.

OVERALL IMPACT

We have identified a novel cell division factor that has not been studied extensively in *S. aureus*. We found that the overexpression of *gpsB*^{Sa} resulted in cell enlargement and many of these enlarged cells lacked division septa. We also observed that depletion of *gpsB*^{Sa} leads to cell lysis and that cells improperly segregate DNA. These results show that GpsB^{Sa} is essential in *S. aureus* and our data provides insight into the interaction partners GpsB^{Sa} utilized to affect cell division. By pursuing the experiments listed in the future directions, we will be able to make a strong contribution to our understanding of cell division regulation in *S. aureus*.

REFERENCES

1. Margolin, W., *FtsZ and the Division of Prokaryotic Cells and Organelles.* Nature reviews. Molecular cell biology, 2005. **6**(11): p. 862-871.
2. Mukherjee, A. and J. Lutkenhaus, *Dynamic assembly of FtsZ regulated by GTP hydrolysis.* The EMBO Journal, 1998. **17**(2): p. 462-469.
3. Nogales, E., et al., *Tubulin and FtsZ form a distinct family of GTPases.* Nat Struct Mol Biol, 1998. **5**(6): p. 451-458.
4. Monahan, L.G., et al., *Division site positioning in bacteria: one size does not fit all.* Frontiers in Microbiology, 2014. **5**: p. 19.
5. de Boer, P.A.J., *Advances in understanding E.coli cell fission.* Current opinion in microbiology, 2010. **13**(6): p. 730-737.
6. Hu, Z. and J. Lutkenhaus, *Topological regulation of cell division in Escherichia coli involves rapid pole to pole oscillation of the division inhibitor MinC under the control of MinD and MinE.* Mol Microbiol, 1999. **34**(1): p. 82-90.
7. Thanbichler, M., *Synchronization of Chromosome Dynamics and Cell Division in Bacteria.* Cold Spring Harbor Perspectives in Biology, 2010. **2**(1): p. a000331.
8. Bernhardt, T.G. and P.A. de Boer, *SlmA, a nucleoid-associated, FtsZ binding protein required for blocking septal ring assembly over Chromosomes in E. coli.* Mol Cell, 2005. **18**(5): p. 555-64.
9. Wu, L.J. and J. Errington, *Nucleoid occlusion and bacterial cell division.* Nat Rev Micro, 2012. **10**(1): p. 8-12.

10. Cho, H., et al., *Nucleoid occlusion factor SlmA is a DNA-activated FtsZ polymerization antagonist.* Proc Natl Acad Sci U S A, 2011. **108**(9): p. 3773-8.
11. Schumacher, M.A. and W. Zeng, *Structures of the nucleoid occlusion protein SlmA bound to DNA and the C-terminal domain of the cytoskeletal protein FtsZ.* Proceedings of the National Academy of Sciences, 2016. **113**(18): p. 4988-4993
12. Marston, A.L., et al., *Polar localization of the MinD protein of Bacillus subtilis and its role in selection of the mid-cell division site.* Genes Dev, 1998. **12**(21): p. 3419-30.
13. Edwards, D.H. and J. Errington, *The Bacillus subtilis DivIVA protein targets to the division septum and controls the site specificity of cell division.* Mol Microbiol, 1997. **24**(5): p. 905-15.
14. Eswaramoorthy, P., et al., *Cellular architecture mediates DivIVA ultrastructure and regulates min activity in Bacillus subtilis.* MBio, 2011. **2**(6): p. e00257-11.
15. Patrick, J.E. and D.B. Kearns, *MinJ (YvjD) is a topological determinant of cell division in Bacillus subtilis.* Mol Microbiol, 2008. **70**(5): p. 1166-79.
16. Pinho, M.G., M. Kjos, and J.-W. Veening, *How to get (a)round: mechanisms controlling growth and division of coccoid bacteria.* Nat Rev Micro, 2013. **11**(9): p. 601-614.
17. Pinho, M.G. and J. Errington, *A divIVA null mutant of Staphylococcus aureus undergoes normal cell division.* FEMS Microbiol Lett, 2004. **240**(2): p. 145-9.
18. Tavares, J.R., et al., *Cytological characterization of YpsB, a novel component of the Bacillus subtilis divisome.* J Bacteriol, 2008. **190**(21): p. 7096-107.
19. Adams, D.W., L.J. Wu, and J. Errington, *Nucleoid occlusion protein Noc recruits DNA to the bacterial cell membrane.* The EMBO Journal, 2015. **34**(4): p. 491.
20. Veiga, H., A.M. Jorge, and M.G. Pinho, *Absence of nucleoid occlusion effector Noc impairs formation of orthogonal FtsZ rings during Staphylococcus aureus cell division.* Molecular Microbiology, 2011. **80**(5): p. 1366-1380.
21. Claessen D, et al., *Control of the cell elongation-division cycle by shuttling of PBP1 protein in Bacillus subtilis*. Mol Microbiol, 2008. **68**(4): p. 1029-1046.

22. Rismondo J, et al., *Structure of the bacterial cell division determinant GpsB and its interaction with penicillin-binding proteins*. Mol Microbiol, 2016. **99**(5): p. 978-998.

23. Swaminathan, B. and P. Gerner-Smidt, *The epidemiology of human listeriosis.* Microbes and Infection, 2007. **9**(10): p. 1236-1243.

24. Mukherjee, K., et al., *Galleria mellonella as a model system for studying Listeria pathogenesis.* Appl Environ Microbiol, 2010. **76**(1): p. 310-7.

25. Gillespie, S.H., *Aspects of pneumococcal infection including bacterial virulence, host response and vaccination.* J Med Microbiol, 1989. **28**(4): p. 237-48.

26. Land AD, et al., *Requirement of essential Pbp2x and GpsB for septal ring closure in Streptococcus pneumoniae* D39. Mol Microbiol, 2013. **90**(5): p. 939-955.

27. Lleo, M.M., P. Canepari, and G. Satta, *Bacterial cell shape regulation: testing of additional predictions unique to the two-competing-sites model for peptidoglycan assembly and isolation of conditional rod-shaped mutants from some wild-type cocci.* J Bacteriol, 1990. **172**(7): p. 3758-71.

28. Fleurie, A., et al., *Interplay of the serine/threonine-kinase StkP and the paralogs DivIVA and GpsB in pneumococcal cell elongation and division.* PLoS Genet, 2014. **10**(4): p. e1004275.

29. Manuse, S., et al., *Role of eukaryotic-like serine/threonine kinases in bacterial cell division and morphogenesis.* FEMS Microbiol Rev, 2016. **40**(1): p. 41-56.

30. Burnside, K. and L. Rajagopal, *Regulation of prokaryotic gene expression by eukaryotic-like enzymes.* Current opinion in microbiology, 2012. **15**(2): p. 125-131.

31. Cousin, C., et al., *Protein-serine/threonine/tyrosine kinases in bacterial signaling and regulation.* FEMS Microbiology Letters, 2013. **346**(1): p. 11-19.

32. Dworkin, J., *Ser/Thr phosphorylation as a regulatory mechanism in bacteria.* Current opinion in microbiology, 2015. **24**: p. 47-52.

33. Wright, D.P. and A.T. Ulijasz, *Regulation of transcription by eukaryotic-like serine-threonine kinases and phosphatases in Gram-positive bacterial pathogens.* Virulence, 2014. **5**(8): p. 863-885.

34. Foulquier, E., et al., *PrkC-mediated phosphorylation of overexpressed YvcK protein regulates PBP1 protein localization in Bacillus subtilis mreB mutant cells.* J Biol Chem, 2014. **289**(34): p. 23662-9.

35. Gaidenko, T.A., T.J. Kim, and C.W. Price, *The PrpC serine-threonine phosphatase and PrkC kinase have opposing physiological roles in stationary-phase Bacillus subtilis cells.* J Bacteriol, 2002. **184**(22): p. 6109-14.

36. Libby, E.A., L.A. Goss, and J. Dworkin, *The Eukaryotic-Like Ser/Thr Kinase PrkC Regulates the Essential WalRK Two-Component System in Bacillus subtilis.* PLoS Genet, 2015. **11**(6): p. e1005275.

37. Madec, E., et al., *Characterization of a membrane-linked Ser/Thr protein kinase in Bacillus subtilis, implicated in developmental processes.* Mol Microbiol, 2002. **46**(2): p. 571-86.

38. Pompeo, F., et al., *Phosphorylation of CpgA protein enhances both its GTPase activity and its affinity for ribosome and is crucial for Bacillus subtilis growth and morphology.* J Biol Chem, 2012. **287**(25): p. 20830-8.

39. Pompeo, F., et al., *Phosphorylation of the cell division protein GpsB regulates PrkC kinase activity through a negative feedback loop in Bacillus subtilis.* Mol Microbiol, 2015. **97**(1): p. 139-50.

40. Giefing, C., et al., *Discovery of a novel class of highly conserved vaccine antigens using genomic scale antigenic fingerprinting of pneumococcus with human antibodies.* J Exp Med, 2008. **205**(1): p. 117-31.

41. Fleurie, A., et al., *Interplay of the serine/threonine-kinase StkP and the paralogs DivIVA and GpsB in pneumococcal cell elongation and division.* PLoS genetics, 2014. **10**(4): p. e1004275.

42. Av-Gay, Y. and M. Everett, *The eukaryotic-like Ser/Thr protein kinases of Mycobacterium tuberculosis.* Trends Microbiol, 2000. **8**(5): p. 238-44.

43. Sassetti, C.M. and E.J. Rubin, *Genetic requirements for mycobacterial survival during infection.* Proceedings of the National Academy of Sciences, 2003. **100**(22): p. 12989-12994.

44. Kang, C.M., et al., *The Mycobacterium tuberculosis serine/threonine kinases PknA and PknB: substrate identification and regulation of cell shape.* Genes Dev, 2005. **19**(14): p. 1692-704.

45. Gupta, M., et al., *HupB, a nucleoid-associated protein of Mycobacterium tuberculosis, is modified by serine/threonine protein kinases in vivo.* Journal of bacteriology, 2014. **196**(14): p. 2646-2657.

46. Thakur, M. and P.K. Chakraborti, *Ability of PknA, a mycobacterial eukaryotic-type serine/threonine kinase, to transphosphorylate MurD, a ligase involved in the process of peptidoglycan biosynthesis.* Biochemical Journal, 2008. **415**(1): p. 27-33.

47. Santiago, M., et al., *A new platform for ultra-high density Staphylococcus aureus transposon libraries.* BMC Genomics, 2015. **16**: p. 252.

48. Steele, V.R., et al., *Multiple essential roles for EzrA in cell division of Staphylococcus aureus.* Molecular Microbiology, 2011. **80**(2): p. 542-555.

49. Youngman, P., J.B. Perkins, and R. Losick, *Construction of a cloning site near one end of Tn917 into which foreign DNA may be inserted without affecting transposition in Bacillus subtilis or expression of the transposon-borne erm gene.* Plasmid, 1984. **12**(1): p. 1-9.

50. Horsburgh, M.J., et al., *sigmaB modulates virulence determinant expression and stress resistance: characterization of a functional rsbU strain derived from Staphylococcus aureus 8325-4.* J Bacteriol, 2002. **184**(19): p. 5457-67.

51. Gregory, J.A., E.C. Becker, and K. Pogliano, *Bacillus subtilis MinC destabilizes FtsZ-rings at new cell poles and contributes to the timing of cell division.* Genes & development, 2008. **22**(24): p. 3475-3488.

52. Haydon, D.J., et al., *An inhibitor of FtsZ with potent and selective anti-staphylococcal activity.* Science, 2008. **321**(5896): p. 1673-5.

53. Tan, C.M., et al., *Restoring methicillin-resistant Staphylococcus aureus susceptibility to beta-lactam antibiotics.* Sci Transl Med, 2012. **4**(126): p. 126ra35.

54. Pinho, M.G. and J. Errington, *Dispersed mode of Staphylococcus aureus cell wall synthesis in the absence of the division machinery.* Molecular Microbiology, 2003. **50**(3): p. 871-881.

55. Pinho, M.G., H. de Lencastre, and A. Tomasz, *Cloning, characterization, and inactivation of the gene pbpC, encoding penicillin-binding protein 3 of Staphylococcus aureus.* J Bacteriol, 2000. **182**(4): p. 1074-9.

APPENDICES

Copyright Clearance

Approval for use of material included in Figure 2 of this thesis:

JOHN WILEY AND SONS LICENSE
TERMS AND CONDITIONS

Oct 15, 2017

This Agreement between Ms. Catherine Spanoudis ("You") and John Wiley and Sons ("John Wiley and Sons") consists of your license details and the terms and conditions provided by John Wiley and Sons and Copyright Clearance Center.

License Number	4210211488615
License date	Oct 15, 2017
Licensed Content Publisher	John Wiley and Sons
Licensed Content Publication	Molecular Microbiology
Licensed Content Title	Structure of the bacterial cell division determinant GpsB and its interaction with penicillin-binding proteins
Licensed Content Author	Jeanine Rismondo,Robert M. Cleverley,Harriet V. Lane,Stephanie Großhennig,Anne Steglich,Lars Möller,Gopala Krishna Mannala,Torsten Hain,Richard J. Lewis,Sven Halbedel
Licensed Content Date	Dec 18, 2015
Licensed Content Pages	21
Type of use	Dissertation/Thesis
Requestor type	University/Academic
Format	Electronic
Portion	Figure/table
Number of figures/tables	1
Original Wiley figure/table number(s)	Figure 8 (A-B)
Will you be translating?	No
Title of your thesis / dissertation	Cell Division Regulation in Staphylococcus aureus
Expected completion date	Dec 2017
Expected size (number of pages)	70